Chapter 6
Dynamic Loading

Christian Meyer[1], Rene de Borst[2], Nenad Bicanic[3],
Filip C. Filippou[4], Koichi Maekawa[5]

Abstract

This chapter deals with those problems of finite element analysis of concrete structures, which arise from the dynamic nature of loadings. Following a short enumeration of the dynamic load categories that are of interest to engineers, the various rate-dependent material models are summarized. The discussion of member models is subdivided into micro and macro finite element models and the different kinds of models for frame elements (plastic hinge and fiber models), together with their hysteresis models for cyclic loads, and some comments on bond-slip and shear effects. Several numerical aspects of dynamic analysis are adressed, and a few examples conclude this chapter.

## 6.1 Introduction

Most loads acting on structures, with the exception of most gravity loads, are of dynamic nature. The judgment whether the dynamic or time-dependent effect of a particular loading can be neglected or not is one of the most basic ones facing the structural analyst. It requires an understanding of the principles of structural dynamics as well as practical experience with the dynamic response of the type of structures to be analyzed (Meyer 1987a). The dynamic analysis of structures is more difficult and expensive than static analysis, and it should be performed only by personnel having an adequate educational background and experience.

[1] Professor, Columbia University, New York, NY 10027

[2] Professor, Delft University of Technology, Postbus 5048, 2600 GA Delft, The Netherlands

[3] Professor, University College, Swansea, Singleton Park, Swansea, United Kingdom

[4] Professor, University of California, 731 Davis Hall, Berkeley, CA 94720

[5] Professor, Asian Institute of Technology, G.P.O. Box 2754, Bangkok, Thailand

Dynamic loads can be subdivided into two categories, according to the kind of effects they have on the behavior of structures:

1. The first category contains loads with sufficiently high strain rates so that the material properties of both concrete and steel are markedly affected. Blast and impact loads clearly belong into this category, whereas the strain rates associated with earthquake, wind, and normal service type loads have generally only moderate influence on the basic material properties. The material behavior characteristics under extremely slow loading rates (creep) are covered in Chapter 5 and will not be addressed here.

2. The second category includes all those dynamic loads not covered in the first category, i.e., it contains all those loads with strain rates low enough to have negligible impact on the material properties. An important role in this category is played by loads of cyclic nature (earthquake and wind, e.g.) that may involve many load reversals. Because of the strain-rate assumption, it is permissible to convert the inertia and damping effects to equivalent static loads and thereby reduce the dynamic analysis problem to an equivalent quasi-static analysis problem, even in the case of load reversals. But as reinforced concrete experiences cracking under load, especially if the reinforcement is strained beyond the yield point, it suffers both strength and stiffness degradation under repeated load applications. Realistic numerical simulation of this behavior using mathematical models poses a challenge of considerable difficulty.

In the next section we shall classify in some additional detail the various dynamic loading types to which concrete structures may be subjected. Section 3 contains a survey of material models that are available for the two main categories mentioned above. Member models are discussed in Section 4. These are models suitable for either micro- or macro-elements in finite element analysis. Section 5 addresses some numerical aspects of dynamic analysis. Several practical application examples are given in Section 6, followed by some conclusions and practical guidelines for engineers, who are contemplating the dynamic analysis of reinforced concrete structures.

## 6.2 Dynamic Loads

In order to justify the added expense of a dynamic analysis, the loading for which the structure response is to be determined has to have at least one of the following characteristics:

a) a loading or strain rate high enough to markedly affect the material properties;
b) a history rich in frequencies that can excite dynamic response;
c) a number of load reversals that lead to damage accumulation, which expresses itself in the form of material deterioration.

Loads due to moving traffic, such as on highway bridges, have a dynamic component which is typically small compared with the static component. In design practice, the dynamic effect is therefore generally accounted for by multiplying the static load with an impact factor. Moreover, since traffic loads are typically service-type loads, reinforced concrete structures are not supposed to respond to them nonlinearly. Therefore, we shall not consider here any kind of

service loads.

The ground motions resulting from destructive earthquakes can subject reinforced concrete structures to very large forces. In fact, current design practice tends to avoid resisting these forces in the linear elastic range and permits preselected structural components to undergo large inelastic deformations under controlled conditions, thereby dissipating large amounts of energy. A considerable body of knowledge exists both on the behavior of concrete structures under earthquake loads and on how to model this behavior for numerical simulation (Paulay and Priestley 1992; ACI-ASCE 1988, 1991; Naeim 1989).

The strain-rate effect of earthquake loads on the material properties is not very significant. It has been reported to be at most as high as 20% (Mahin and Bertero 1972). Yet, Yokoyama et al (1990) showed that the rate effect causes noticeable differences between pseudo-dynamic and real dynamic tests of concrete columns. Several authors have reported comparable effects of the loading rate on strength properties and energy absorption of frame members and shear walls (Okada et al 1989; Song and Maekawa 1991; Endoh et al 1989).

The other two criteria listed above (frequency content and load reversals) are clearly met by earthquake-type loadings. Because of the randomness of seismic ground motions, the frequency content can show considerable variability, so that the threat of resonant amplification plays an important role in earthquake-resistant design. And the number of load reversals can be considerable: the 1985 Mexico City earthquake caused almost 20 full load reversals of a strongly harmonic nature. The strength and stiffness degradation that concrete structures experience under such loading can be accompanied by extensive damage if not failure. The redistribution of stresses in such a deteriorating structure, coupled with the extreme randomness of earthquake ground motions, poses an enormous challenge to the analyst who wishes to simulate this behavior numerically in order to make rational reliability and survivability assessments.

Wind loadings are generally decomposed into a mean static pressure plus pressure fluctuations which oscillate about the mean. Unless severe resonant amplification occurs, e.g. due to vortex shedding in certain steady-state winds, concrete structures are seldom expected to respond nonlinearly. The strain rates associated with wind loads are of the same order as those of earthquake ground motions, i.e., they do not alter significantly the material properties. Even though the number of load cycles can be very large, the low vibration amplitudes are generally not cause of any fatigue-type material degradation. Thus, wind is not an important load within the context of our discussion here.

Blast loads and missile impact cause very high strain rates. Blast loading results from either internal or external explosions. Impact loading can be caused by missiles such as military projectiles or tornado-borne debris, fragments of a fractured turbine, high-energy pipe ruptures, or various collision scenarios. All of these cases have in common a very short but intense load impulse, i.e. load reversals are rarely involved, and also resonant amplification is not as critical as in the case of repeated load applications. But the inertia effects are extremely important, and because of the high strain rates, which strongly affect the material properties, equivalent quasi-static analysis is generally not possible.

In sum, the models to be described below have been developed either for

earthquake response analysis or for applications involving blast or impact loads.

## 6.3 Material Models

### 6.3.1 General

Material models for plain or reinforced concrete responding to both static and monotonic load are covered in detail in other chapters of this report, notably in Chapter 2. If the loading is of a dynamic nature such that either the strain rates are significant, or load reversals into the inelastic range are involved, then those models are not applicable without special modifications.

In this section, first an overview will be given of rate-dependent models which are often adjustable to either very high or very low strain rates. Next we shall summarize recent advances in damage mechanics, which is a very useful tool for modeling the strength and stiffness degradation of reinforced concrete under cyclic loading.

### 6.3.2 Rate-Dependent Models

a) Introduction

The stress- or strain-rate dependence of concrete behavior is well documented. Experiments are conducted mainly on uniaxial compression or tension samples, but also more complex stress histories have been studied recently. The most prominent feature is the significant increase in strength and Young's modulus, as the average rate of straining increases from the quasi-static rate (approximately $10^{-3}/sec$) to the very high strain rates associated with impact conditions (approximately $10^{2}/sec$), Fig. 6.1. Going from one to the other extreme within this range, concrete can double its strength. This factor cannot be ignored in realistic analyses. As most experiments are conducted on plain concrete or steel samples, mathematical models for reinforced concrete usually combine response features of the constituent materials.

Other chapters of this report deal with concrete modeling within the elasto-plastic framework, and a number of yield or failure surfaces have been mentioned. In the simplest format, these hypersurfaces describe the union of various stress states, for which concrete behavior ceases to be elastic and some non-recoverable deformation takes place. Of the various reference frames, the principal stress space is the most common one to denote a stress point.

Regardless of whether these surfaces have been described mathematically by some kind of curve fitting technique, or they represent a visualization of an integral theory (like Mohr-Coulomb), a typical surface is cone-like and pressure dependent. Many different surfaces have been proposed, which are more or less sophisticated, and more or less convenient for computational purposes. The implementation of such models within finite element analysis and flow theory of plasticity requires the definition of a plastic strain tensor increment (usually defined by a so-called plastic potential surface in the same principal stress space, and its gradient), and accounting for any changes that the surface may undergo as a result of hardening or softening during the increment (so-called consistency condition). Various computational algorithms for the stress increment computa-

tion iterate to satisfy both global equilibrium and to ensure that the stress and strain states at all integration points correspond to the elasto-plastic constitutive law. By definition, there is no *real time* involved in finite element analysis with plasticity. All inelastic processes are assumed to have sufficient time to develop, as if everything is happening at an infinitely slow time rate. However, often "time steps" are mentioned in the context of plasticity computations, but these refer to a "pseudo-time" and should never be confused with real time.

It is precisely this issue that makes modeling of rate-dependent concrete behavior so fundamentally different from modeling its static behavior. Failure surfaces are now rate dependent. They may expand or shrink, depending on what rate a material point experiences. For a finite element model of some concrete structure under impact loading, for example, the various integration points may be instantaneously subject to vastly different stress or strain rates, which in turn correspond to vastly different instantaneous failure surfaces.

It is not straight-forward to define an appropriate measure of stress or strain rate for multiaxial states in order to relate it to experimental data, that are almost invariably based on one-dimensional samples and simple stress states.

Clearly, the inclusion of the *real time* plays a crucial role here. Inelastic processes cannot develop in concrete in fast-rate situations, prior to some change of overall loading rate and, consequently, the change of the instantaneous failure surface. In modeling terms, it is not possible to use a traditional time-independent plasticity framework in such situations.

In the following, several possibilities will be discussed to model the strain-rate dependency within the elasto-plastic, elasto-viscoplastic, and fracture mechanics frameworks.

b) Approximation of Rate-Dependency in Elasto-Plasticity

A crude approximation of the rate dependency may be obtained by adjusting the elasto-plastic failure surface parameters so that they correspond to some average rate - typically to increase the failure surface by some arbitrary scaling. Such a model is clearly a poor approximation. As the rate of process cannot be defined a priori, it is also neither constant in time, nor is it uniform within the structure. In fact, the rate of inelastic straining can be vastly different from one integration point to another, and the modeling could be improved by employing for every integration point an instantaneous failure surface (Nilsson 1978), which depends on the instantaneous strain rate at that point. This means that the failure surfaces are allowed to "breathe", i.e. to soften or harden for a given instant in real time, so-called *rate-hardening* or *softening*, dependent on some measure of strain rate. The model response becomes strain-rate dependent, although in principle still an elasto-plastic model, where all iterative stress increment computations have to be performed in some *dummy* time, and the *real* time computation can continue only when the apparent steady state is reached for the current position of failure surfaces. There are various possible measures of strain rate, but it is difficult to apply the instantaneous rate-hardening concept, as the rate of straining may fluctuate within the stress increment computation, and convergence may be problematic.

A model proposed recently by Chappuis and Bachmann (1988) utilizes the

Chen-Chen surface description, and the surface is made rate-dependent by relating residual strengths $f_t$ and $f_c$ (used for an instantaneous surface description) to the current strain rate. A linear relationship between the strength and the logarithm of the strain rate is adopted, with an upper and lower bound. In order to decide on the current rate of straining in multiaxial situations at a given integration point, a maximum strain rate along one of the principal strain axes is chosen as an indicator of the rate of process, i.e.

$$\dot{\epsilon} = \max(\dot{\epsilon}_1, \dot{\epsilon}_2, \dot{\epsilon}_3)$$

c) Elasto-Viscoplastic Models

A more appropriate mathematical framework is found in elasto-viscoplasticity theory, which has been used by various researchers for developing rate-dependent concrete models.

The elasto-viscoplastic model, proposed by Perzyna (1966), differs from the elasto-plastic model insofar, that the stress point can be outside the elastic limit surface. The elasto-plastic model recognizes stress states only within and on the yield surface, and most of the computational effort is spent to return the stress point onto a current yield surface. In an elasto-viscoplastic model, the rate of inelastic flow is defined as some function of the distance between the stress point and the elastic limit surface and the so-called fluidity parameter $\gamma$,

$$\dot{\epsilon}_{ij}^{vp} = \gamma < \Phi(F) > \partial F / \partial \sigma_{ij} \qquad (6-1)$$

where the dot ( $\dot{}$ ) defines the rate with respect to time, and the $< >$ bracket implies that the expression is activated only if $F > 0$, i.e., when the stress point is outside the elastic limit surface. If an elasto-viscoplastic model is adopted within the proper context of real time (rather than as an artifice to obtain steady-state plasticity solutions, i.e. as a stress-return algorithm), the response becomes, by definition, rate dependent, i.e. it will change as a function of loading rate. The adoption of such a model to concrete requires the definition of, 1) some elastic limit surface (sometimes also called a discontinuity surface), 2) the fluidity parameter, and 3) the functional relationship $< \Phi(F) >$.

To choose an elastic limit surface is relatively easy, as any convenient failure surface description could be used, with proper scaling, since one is dealing with the elastic limit surface, rather than the failure surface. The other two model parameters, the fluidity parameter and the functional relationship for $\Phi(F)$ should ideally be obtained from three-dimensional experiments conducted under different rates of loading. As such experiments are scarce even for uniaxial compression, the models that are in use aim to reproduce one-dimensional responses and assume correct behavior for other stress histories.

Probably the most complete rate-sensitive model for concrete has been suggested by Nilsson (Nilsson 1978; Nilsson and Glemberg 1981), who introduced an elasto-viscoplastic-plastic-brittle model for concrete at high rates of loading. The model is essentially an elasto-viscoplastic model, where the closed elastic limit surface is defined by a generalized ellipsoidal surface

$$F = \left[ \left( \frac{\frac{2\sigma_a}{H_r} - \xi_u - \xi_l}{\xi_u - \xi_l} \right)^2 + \left( \frac{\frac{\tau_a}{H_r}}{b(\theta)} \right)^2 \right]^{1/2} - 1 \qquad (6-2)$$

where $\sigma_o$, $\tau_o$ are the octahedral normal and shear stress, and $\theta$ the Lode angle of similarity. $\xi_u$ and $\xi_l$ are surface intersections with the space diagonal, Fig. 6.2. The hardening parameter $H_r$ indicates the change of the elastic limit surface as a result of inelastic processes. Nilsson uses the hardening parameter also to model the so-called rate hardening, where the normalized hardening for the uniaxial compressive strength $f_{cu}$ is obtained by curve fitting of uniaxial experimental data,

$$\frac{H_r}{f_{cu}} = c_1 + c_2\, ln(\dot{\epsilon}_{ef}) + c_3\, [ln(\dot{\epsilon}_{ef})]^2 \qquad (6-3)$$

with $c_1 = 1.6$, $c_2 = 0.104$, and $c_3 = 0.0045$.

For multiaxial cases, a scalar measure of the process rate, the "effective strain rate", $\epsilon_{ef}$, is assumed to be given by the root mean square of the normal and shear octahedral strain rates,

$$\dot{\epsilon}_{ef} = \left(\dot{\epsilon}_o^2 + \frac{1}{4}\dot{\gamma}_o^2\right)^{\frac{1}{2}} \qquad (6-4)$$

Nilsson also made the fluidity parameter $\gamma$ dependent on the effective strain rate, by the following function,

$$\gamma(\dot{\epsilon}) = \dot{\epsilon}_{ef}\, e^{-r ln|\frac{\dot{\epsilon}_{ef}}{\dot{\epsilon}^r_{ef}}|} \qquad (6-5)$$

where $\dot{\epsilon}^r_{ef}$ is the reference value for the effective strain rate, and $r$ is a material constant. The adopted value for $\dot{\epsilon}^r_{ef}$ was typically $2.0 \times 10^{-6}$ (quasi-static rate), and the appropriate value for the coefficient $r$ was found to be 0.0625.

For the functional relationship $\Phi(F)$, Nilsson adopted the exponential function of a form suggested by Perzyna,

$$\Phi(F) = \left(\frac{F}{F_o}\right)^{\alpha} \qquad (6-6)$$

and the appropriate value for $\alpha$ to fit the experiments was found to be 0.40.

Finally, Nilsson introduced the strain-rate dependency of the outer (failure) surface, in the context of instantaneous rate hardening. Two parts of the failure surface, covering the tension/compression and tension/tension regime, are allowed to harden or to soften (Nilsson 1978), depending on the instantaneous effective strain rate.

Other investigators followed similar lines in developing rate-dependent models for plain concrete. Bicanic (1978; Bicanic and Zienkiewicz 1983) proposed a multi-axial elasto-viscoplastic degradation model, Fig. 6.3, in which only the fluidity parameter was elastic strain-rate dependent, and the elastic limit Mohr-Coulomb-like surface (discontinuity surface) was kept constant in the pre-failure regime. The rate dependence of the fluidity parameter was approximated on the basis of Hatano and Tsutsumi's tests (1960),

$$\gamma(\dot{\epsilon}) = 10^{-a_0}(\epsilon_{el})^{a_1} \qquad (6-7)$$

The parameters $a_o$ and $a_1$, found by curve fitting for various concrete qualities, ranged from 2.20 to 2.90 and from 0.72 to 0.78, respectively. These values are valid for strain rates in the range of $10^{-4}$ to $10^{-1}/sec$. In addition, the transition to the post-failure regime (modeled by the rapidly softening elastic limit surface, and hence accelerating the rate of inelastic flow, as the stress point is at a greater distance) is initiated when the stress point reaches a strength limit surface. This strength limit surface shrinks as a result of accumulated inelastic work (i.e. it is a degrading, inelastic "work-softening" surface), and it serves here as a monitoring device to indicate failure.

Such a format allows the model to recognize the rate dependence of strength via the accumulated inelastic work. For high rates of loading, there is little time for inelastic work to develop, the strength limit surface does not shrink much, and higher strength results. For lower loading rates, there is sufficient time for inelastic work to develop, which in turn reduces the strength limit surface. A Mohr-Coulomb-like surface has been used for the strength limit surface, and surface parameters were based on the uniaxial compression and tension experiments conducted under various loading rates. The two degradation functions that define the reduction of the uniaxial compression and tensile strengths, $f_{cu}$ and $f_t$, as functions of the accumulated inelastic work, control the shrinking of the strength limit surface as well. There is a direct coupling between the inelastic work in tension and compression, as both strength limit surface parameters are affected by the accumulated inelastic work, irrespective of which response regime causes the damage. At any given time, the multiaxial strain state was mapped into an equivalent uniaxial measure for the rate of process through the backward difference approximation of the second elastic strain invariant,

$$\dot{\epsilon}(t) \approx J_2(\dot{\epsilon}_{el_t}) \approx \frac{1}{\Delta t}[J_2(\epsilon_{el_t}) - J_2(\epsilon_{el_{t-\Delta t}})] \qquad (6-8)$$

Similar degradation concepts have been adopted by Meyer and Delgado-Saavedra (1986; Delgado 1985), who extended and improved the original model of Bicanic (1978) by replacing the Mohr-Coulomb-like surfaces by the five-parameter model surface proposed by Willam and Warnke (1974) to describe both the discontinuity and strength limit surfaces, Fig. 6.4. The model was calibrated, for fast loading rates only, against the test results reported by Hatano and Tsutsumi (1960). The strain-rate dependence of the fluidity parameter was determined as

$$\gamma = e^{-8.46}[\dot{J}_2(\epsilon_{el})]^{-0.0593} \qquad (6-9)$$

The degradation of the tension and compression meridians of the strength limit surface are suitably controlled by the two degradation functions. The multiaxial states are mapped into the equivalent uniaxial state in the same way as in the original model (Bicanic and Zienkiewicz 1983). The model has been applied to the three-dimensional stress analysis of concrete specimens.

The rate sensitivity in both Bicanic's and Delgado-Saavedra's model is introduced on two levels: the fluidity parameter is strain-rate dependent, and the degrading strength limit surface ensures the rate-dependence of the failure stress level.

None of the models proposed to date considers the fact that the elastic modulus is affected by the strain rate.

d) Fracture Mechanics Models

Concrete cracking models based on fracture mechanics employ either the fracture energy release rate $G_f$ (fracture energy models) or the fracture toughness $K_{Ic}$ (linear elastic fracture mechanics models). Both parameters are strain-rate dependent, and numerous tests (Reinhardt 1986; Bruhwiler 1990) have confirmed that there is an increase of both $G_f$ and $K_{Ic}$ with increased strain rate.

The most recent set of strain-rate dependent fracture properties of concrete needed for fracture mechanics models was defined by Bruhwiler (1990), who proposed a general power law to fit experimental data. Typical expressions for strain-rate dependent concrete fracture properties as a function of so-called relative strain $\dot{\epsilon}_r$, or deformation rate $\dot{v}_r$, (the ratio between the dynamic and static strain or deformation rate) are given as,

$$\begin{aligned} \text{uniaxial tension}: \quad f_t &= f_{t0}(\dot{\epsilon}_r)^{0.081} \\ \text{elastic modulus}: \quad E_t &= E_{t0}(\dot{\epsilon}_r)^{0.020} \\ \text{fracture energy release rate}: \quad G_f &= G_{f0}(\dot{v}_r)^{0.048} \\ \text{fracture toughness}: \quad K_{Ic} &= K_{Ic0}(\dot{v}_r)^{0.034} \end{aligned}$$

These strain-rate dependent properties can be utilized in any concrete model that employs fracture properties, Fig. 6.5, such as fracture-based softening plasticity.

Mixed-mode rate-sensitive fracture models are still in their infancy, although the experimental evidence (John and Shah 1990) suggests that the usually favorable rate effects (such as strength increase) may be counteracted by the change from a ductile to a brittle mode of material failure.

### 6.3.3 Modeling of Damage Due to Cyclic Loading

Concrete is known to deteriorate both in strength and stiffness under repeated load applications, especially if it is stressed well beyond half its uniaxial strength in compression or to its rupture modulus in tension. The gradual accumulation of damage up to failure is basically a fatigue phenomenon, and within the context of our discussion, a low-cycle fatigue problem. Both from a modeling and design standpoint, it is important to distinguish between the fundamentally different mechanisms of damage accumulation under monotonic and repeated load application, especially if load reversals are involved.

First, it is essential to introduce a useful and rational definition of damage. The concept of damage is all-pervasive in structural engineering, and there have been numerous proposals to define it (Chung et al. 1987; Reitherman 1985). Most of these are of a more or less empirical nature, for example those intended for post-earthquake inspections and therefore prone to subjective influences on the part of the inspectors. To avoid that problem, Chung et al. (1987, 1989) have approached the damage definition by tieing it to the degree of physical deterioration with clearly defined consequences regarding the material's capacity to resist further load. Similarly, the notion of failure has to be stripped of its common arbitrary definition (on the member or structural level) by relating it to a specific level of damage at which the material ceases to resist further load. Meyer (1991) proceded to define a damage index $D$ as the ratio between the

energy dissipated up to a certain point, $E_i$, and the total energy dissipation capacity, $\overline{E}_i$,

$$D = \frac{E_i}{\overline{E}_i} \qquad (6-10)$$

This definition can be substituted for the cycle ratio $(n_i/N_i)$ used in conventional fatigue analysis and is readily applicable to plain concrete. Failure is defined as the point at which the slope of the stress-strain curve ceases to be positive. The energy dissipation capacity is clearly a function of stress or strain level.

Other suggested definitions of material damage are total strain accumulation (Holmen 1982) and stiffness as measured in ultrasonic tests (Suaris and Fernando 1987).

Any realistic analysis of reinforced concrete structures for cyclic load is contingent upon a material model which correctly reflects the damage accumulation of concrete under repeated load application. The problem is that the data base needed to develop such a model is extremely scarce. S-N curves have been generated for some selected cases (Shah 1982), but for the low-cycle fatigue range that is of interest for earthquake response analysis, very few data exist. Grzybowski and Meyer (1991) have initiated a testing program for both plain and fibre-reinforced concrete. Some of the preliminary data are shown in Fig. 6.6. The damage accumulation curves reproduced in Fig. 6.7 clearly deviate from the straight line corresponding to Minor's hypothesis. But because of the different damage definition, they do not have the same shape as the curves reported by Holmen (1982), with their characteristic inflection points. Oh (1991) has proposed a damage accumulation law by fitting cubic polynomials to Holmen's data. Efforts are under way at Columbia University to expand the needed experimental data base and to derive from it a damage accumulation law that can be combined with any of the material models discussed earlier.

Continuum damage theory, which forms the basis of several damage models, was first developed by Kachanov (1958). He introduced a voids ratio in a given cross-sectional area as damage variable, which varies from 0 for a virgin material to a critical value for a cracked material. Mazars (1981; Mazars and Pijaudier-Cabot 1989) developed the concept further and applied it to concrete. Krajcinovic and Fonseka (1981a,b) used a vectorial damage approach to describe concrete damage. A similar damage model for brittle solids was proposed by Suaris and Shah (1984, 1985) and applied to dynamic loading. The damage vector introduced in these models represents the area density of the microcracks and is perpendicular to the microcrack plane. The constitutive equations are derived from the thermodynamic potential Helmholtz free energy. The number of free constants to be determined in these models is quite large, and their determination requires further assumptions. The model of Mazars and Pijaudier-Cabot (1989) was derived within the framework of the thermodynamics of irreversible processes, assuming that only the elastic properties of the material are affected by damage. Chen and Buyukozturk (1985) proposed a rate-independent damage-type constitutive model for multiaxial cyclic loading. These damage models have yet to be implemented in general finite element codes for the dynamic analysis of actual concrete structures.

## 6.4 Member Models

### 6.4.1 General

In this section recent developments in the modeling of reinforced concrete members under dynamic loads will be discussed. It covers *microscopic* and *macroscopic* elements as well as *frame element* idealizations. Since the modeling of reinforced concrete structures under monotonic loads was discussed in earlier chapters of this report, only issues related to the dynamic behavior will be addressed here.

There is some confusion to date as to what constitutes a microscopic and a macroscopic finite element idealization of a structure. We are offering the following definitions: a finite element model which is based on the stress-strain relations of the constituent materials of reinforced concrete and their interactions is regarded as *microscopic*, while a model which treats reinforced concrete as a new composite material with its own composite stress-strain relation is defined as *macroscopic*. Even though these definitions might appear arbitrary at first, it is clear that the second approach permits the modeling of entire panels under relatively uniform stress or strain states, using a single macro- or superelement. This is not feasible with the first approach.

The distinction between a macroscopic finite element and a frame element model is that the former is based on a composite stress-strain relation, while the latter makes use of simplifying assumptions regarding the kinematics of member deformations. In the case of fiber models the behavior is derived from the uniaxial stress-strain relations of a number of fibers at several sections along the member length, while plastic hinge models are based on the moment-curvature relation at several critical sections or even the moment-rotation relation for the ends of the entire member.

The use of microscopic finite element models in the dynamic analysis of large RC structures is limited in practice for several reasons:

1. The computational cost is very high, and even present-day computers require excessive time to solve structural problems of moderate or large size.
2. The material behavior of concrete under biaxial and triaxial cyclic loading conditions is still not well understood and few models of such behavior are presently available. The most promising of these models are discussed in Section 4.3.
3. The designer, who wishes to use the results of a nonlinear dynamic analysis, is interested mostly in member deformations -usually rotations- and forces, which he expects to obtain without the need to evaluate enormous amounts of output.

By contrast, microscopic finite element models are best suited to address local detailing problems, such as the behavior of reinforcing bar anchorages under cyclic loading conditions. In this context it is important to develop computer analysis systems which permit the seamless integration and exchange of data between refined local models and global element models.

### 6.4.2 Micro Finite Element Models

As defined here, microscopic finite element models attempt to describe the dynamic behavior of reinforced concrete elements by the simple superposition of the material matrices for plain concrete, reinforcing steel and their interaction through bond-slip along the bar and shear-sliding along cracked surfaces. Even though some models of the cyclic behavior of plain concrete, reinforcing steel, bond-slip and shear-sliding have been proposed, virtually no studies have attempted to include all these effects to model the dynamic behavior of reinforced concrete structures. Investigators have usually isolated the one or the other effect and have tested their models under relatively simple stress or strain fields. Even so, the success of such studies has been rather limited for the following reasons:

1. The cyclic behavior of plain concrete under general two- and three-dimensional load histories is not well understood to date, and few analytical models have proven adequate for all possible loading histories. The recently proposed micro-plane model (Bazant and Ozbolt 1989) holds some promise to satisfy this need.
2. The bond between reinforcing steel and concrete under dynamic loading conditions has been studied only under ideal conditions, and little is known about this behavior under general conditions of cover, distance to the crack, etc. This is also true for the shear transfer across cracked surfaces where the behavior is affected by the amount of reinforcing steel, the angle between reinforcing bars and the crack, etc. Further experimental studies are urgently needed.

Another difficulty of this modeling approach is that the introduction of independent models for bond-slip and shear-sliding fits well with a discrete crack modeling approach, which, however, enjoys limited popularity among researchers, regardless of the fact that very little is known about the implementation of disrete crack models under dynamic loading conditions.

A widely used model for the cyclic behavior of plain concrete is the nonlinear orthotropic model of Darwin and Pecknold (1976). In this model the biaxial concrete behavior is derived by modifying the uniaxial stress-strain behavior of concrete, for which a few experimental data and models already exist (Karsan and Jirsa 1969). More complicated models (Meyer and Okamura 1985; IABSE 1987; Chen 1982) seem to suffer from the need for extensive calibration of their parameters.

For the hysteretic behavior of reinforcing steel many models are available, and the reader is referred to the extensive literature survey of the state-of-the-art report (Nilson 1982). It appears, however, that the most suitable model in the finite element context appears to be the one proposed by Menegotto and Pinto (1973).

In a smeared crack modeling approach the bond-slip effect is usually accounted for by means of the double-node concept, where one node is attached to the concrete and the other to the reinforcing steel, and both nodes initially occupy the same place. The nodes are usually connected by bond-link elements (Nilson 1982), even though more general interface elements have also been proposed (Meyer and Okamura 1987). In a recent attempt by Kwak and Filippou (1990) the bar is embedded into the concrete element, but the bond-slip is in-

cluded explicitly in the model. The main difficulty with bond-slip in smeared crack models lies in assigning material properties to the interface elements, when it is known from experiments that the cyclic bond-slip behavior is affected by the distance to the next crack. The effect of variation of bond-slip properties with distance to the next crack has not been explored to date.

A general shear-sliding model in a smeared crack setting, which accounts for deterioration under cyclic loading, has been proposed by Riggs and Powell (1986). Initial results are very encouraging, but the model is computationally expensive and suffers from numerical instability when multiple cracks form at an integration point.

One of the main difficulties with micro finite element models lies in the definition of crack opening and closing at a point, particularly, when multiple cracks form in a smeared crack model. The numerical difficulties which arise from this problem are addressed in a later section of this chapter.

### 6.4.3 Macro Finite Element Models

The strong interaction between reinforcing steel and concrete has convinced researchers that the behavior of reinforced concrete cannot be reproduced by simple superposition of the material matrices for plain concrete and reinforcing steel, with the addition of bond and shear interface elements. In the "smeared" approach, reinforced concrete is treated as a nonhomogeneous continuum with properties which include the effect of cracking, bond-slip of reinforcement and shear-slip along crack surfaces. Such macroscopic models have been developed only for two-dimensional plane stress or plane strain conditions. Since monotonic models of this kind are addressed elsewhere, only two models which specifically address cyclic loading are introduced here.

In the macroscopic finite element approach, the stress-strain constitutive matrix represents the average behavior of some element volume. In this case stresses can be thought of as the loads acting on the element surfaces divided by the corresponding surface areas, and strains are derived from the element deformations divided by the corresponding element dimensions. The material properties of the composite material can be directly derived from experimental results, as exhibited by the well known Toronto tests on panel elements (Collins et al. 1985). Such constitutive relations can be defined as reinforced concrete material models, when derived from small specimen sizes, or reinforced concrete member or superelement models, when derived from large RC panels. In any case the tangent stiffness matrix of the element is derived by superposing the corresponding stiffness matrices for concrete, $K_c$, and reinforcing steel, $K_{si}$, where $i$ represents the direction of a particular reinforcing layer. This superposition takes place after transformation to a global coordinate system,

$$\mathbf{K}_e = \mathbf{T}_c^T \mathbf{K}_c \mathbf{T}_c + \sum_i \rho_i \mathbf{T}_{si}^T \mathbf{K}_s \mathbf{T}_{si} \qquad (6-11)$$

where $\mathbf{T}_c$ and $\mathbf{T}_{si}$ are the transformation matrices for concrete and reinforcing steel, respectively, and $\rho_i$ is the reinforcing ratio of layer $i$ within the volume tributary to the integration point.

In the macroscopic modeling approach the constitutive matrices of concrete and reinforcing steel include the effect of tension stiffening between cracks. In

the models of the Toronto school (Vecchio and Collins 1982; Stevens et al. 1987) this effect is included in the concrete matrix, while the model by Cervenka (1989) accounts for the tension stiffening effect by modifying the matrix for the reinforcing steel.

Under low stresses concrete remains uncracked and exhibits a linear elastic isotropic behavior. The most convenient reference system for describing the behavior of the element in this stress range is that made up by the principal stress directions. Under increasing loads the stress combination in the critical region of the member often reaches the tension-compression branch of the biaxial failure envelope. At this stage a crack is assumed to form perpendicular to the principal tensile stress, and the concrete material stiffness matrix is now based on stress-strain relations for cracked concrete, an orthotropic material. Two basic approaches have crystallized:

a) In the model of Cervenka the crack direction is kept fixed for subsequent loading. The off-diagonal terms of the concrete material matrix are neglected, but the diagonal term corresponding to shear seems to play an important role in the response of the member, particularly in othogonal fixed crack models.
b) The model by Stevens et al. (1987) is an extension of the Modified Compression Field Theory of Vecchio and Collins (1982) into the cyclic loading range. Based on cyclic shear tests on reinforced concrete panels, Stevens et al. assume that the principal directions of the concrete stress increment tensor coincide with those of the strain increment tensor. This model thus belongs to the class of Rotating Crack Models.

In either case the stress-strain behavior in each principal direction is described by uniaxial stress-strain relations, which are modified to account for the effect of stress in the other direction. Some disagreement exists on the magnitude of this effect between researchers at Toronto and others, notably, Mehlhorn and his co-workers (Kollegger and Mehlhorn 1988), who have also conducted panel tests. Also worthy of note is a macroscopic model for shear wall elements by Inoue and Suzuki (1991), derived from a microscopic model using smeared crack finite element analysis.

### 6.4.4 Frame Element Models

Depending on the desired level of detail and, consequently, accuracy we can distinguish two classes of frame member models: plastic hinge models and fiber models. In both cases, the stiffness matrix of an entire member, relating end moments to corresponding end rotations, is established directly by assuming a moment and corresponding curvature distribution and applying the principle of virtual work. Early models assumed all inelastic deformations to be concentrated at the end points in hinges. More recent models permit inelastic deformations to spread into the member.

In a fiber model the member behavior is monitored at a number of sections, which are, in turn, subdivided into a number of layers or fibers. The section stiffness is obtained by integrating the stiffnesses of all layers, and the member stiffness is taken as the weighted integral of the section stiffnesses.

a) Plastic Hinge Models

The very first inelastic girder model was proposed by Clough (1966). In this model, known as the two-component model, a bilinear elastic strain hardening moment-curvature relationship is assumed along the length of the girder. The beam model consists of two components acting in parallel: one which is linear elastic and one which is elastic-perfectly plastic, with the plastic deformations concentrated in plastic hinges at the ends of the element. One of the shortcomings of this model is the difficulty of accounting for the stiffness deterioration of RC elements during cyclic loading. To overcome this problem, Giberson (1969) proposed the so-called one-component model. This consists of two nonlinear rotational springs, which are attached at the ends of a perfectly elastic element. All nonlinear deformations of the element are lumped in the two rotational springs, to which any kind of hysteretic law can be assigned. A different approach to the problem of modeling the seismic behavior of RC frame members was proposed by Otani (1974). He divided the member into a linear elastic and an inelastic element, acting in parallel, with inelastic rotational springs attached at both ends to represent the fixed-end rotations at the beam-column interface due to slip of the reinforcement in the joint. Otani's study was the first to recognize the importance of fixed-end rotations in predicting the seismic response of RC frame structures.

Mahin and Bertero (1976) reviewed the various definitions of ductility factors in earthquake resistant design and discussed the prediction of the rotational ductility demand in structural elements. They pointed out how to modify the ductility factors for a beam represented by a two-component model to match those for a beam in which inelastic deformations spread into the member. Since the two-component model substantially underestimates the post-yielding stiffness of a member, the seismic response of the structure will not be predicted accurately. This is particularly true in the case of local response quantities such as inelastic rotations of girders and joints. It does not, therefore, appear reasonable to estimate ductility requirements of RC frame elements using two-component models.

The effect of axial force on the flexural stiffness of a member was first accounted for in the model proposed by Takayanagi and Schnobrich (1979) in their study of the seismic response of coupled wall systems. The slip of the reinforcing bars anchored in the wall is represented by springs. The effect of shear in the coupling beams is also taken into account. A modified Takeda model is adopted for the hysteretic behavior of the beam elements. The model accounts for the "pinching" effect during reloading and the strength decay due to loss of shear resistance after crack formation and yielding of the reinforcement in the coupling beams. The seismic response of a plane frame coupled with a shear wall was studied by Emori and Schnobrich (1981). They conducted nonlinear static analyses under cyclic load reversals using various different beam models and concluded that a concentrated spring model predicts most satisfactorily the inelastic response of RC girders, while a multiple spring model is needed to accurately describe the inelastic behavior of shear walls. For a detailed study of the inelastic response of plastic zones in columns, the authors recommend the use of a layer model.

A model for the analysis of seismic response of RC structures was proposed by Banon et al. (1981). The one-component model in its original form describes

the nonlinear behavior of the element. The hysteretic moment-rotation relation is based on a modified Takeda model. In order to reproduce the "pinching" effect due to shear and bond deterioration, a nonlinear rotational spring is inserted at each member end. The hysteretic model of the nonlinear springs is based on a bilinear skeleton curve with strength decay under large deformations and pinched shape during reloading. The authors also proposed a set of damage indicators in an effort to quantify the performance of a structure during an earthquake.

An integrated experimental and analytical study on the effect of bond deterioration on the seismic response of RC structures was published by Otani et al. (1985). The one-component model was adopted for frame elements and Takeda's model to describe their hysteretic behavior. A rotational spring at each member end with Takeda-type rules modelled the hysteretic behavior caused by the reinforcement slip due to bond deterioration. No strength decay is introduced in the monotonic skeleton curve, since no appropriate experimental data were available.

A model for assessing structural damage in RC structural elements was proposed by Park and Ang (1985), in which damage is expressed as a linear combination of a deformation ductility ratio and the hysteretic energy absorbed during cyclic load reversals.

The first *spread plasticity* model was introduced by Soleimani et al. (1979). In this model a zone of inelastic deformations gradually spreads from the beam-column interface into the member as a function of loading history. The rest of the beam remains elastic. The fixed-end rotations at the beam-column interface are modeled through point hinges which are inserted at the ends of the member. These are related to the curvature at the corresponding end section through an "effective length" factor which remains constant during the entire response history.

Meyer et al. (1983) developed another spread plasticity model, using the same flexibility coefficients as Soleimani, but they determined the stiffness of the plastic zone during reloading in a different way and combined it with Takeda-type rules to describe the hysteretic behavior. This model does not account for the axial force effect.

In their study of the nonlinear response of plane rectangular frames and coupled shear walls, Keshavarzian and Schnobrich (1984) extended Soleimani's model to column elements, by accounting for the interaction between bending moment and axial force to determine the strength and stiffness of column elements. The study compared various spread plasticity as well as one-component, two-component and multiple spring models. It concluded that the one-component model is well suited for describing the inelastic behavior of RC girders and that the two-component model has the same versatility as the one-component model, yielding similar results. The multi-layer model was found to be very expensive for nonlinear dynamic analysis of multistory structures. Fluctuation of axial forces in coupled shear walls and in exterior columns of frame structures were found to significantly affect the forces and deformations in individual walls and columns.

Roufaiel and Meyer (1987) extended the spread plasticity model to include the effect of shear and axial forces on the flexural hysteretic behavior, using

a semi-empirical set of Takeda-type rules. The predictions of the model were compared with available experimental data and showed very good agreement. A set of new damage parameters was proposed, which seem to correlate well with the residual strength and stiffness of specimens tested in the laboratory.

Finally, Filippou and Issa (1988) subdivided a member into different subelements. Each subelement describes a single effect, e.g. inelastic behavior due to bending, shear behavior at the interface, bond-slip behavior at the beam-column joint. The interaction between these effects is then achieved by combining the subelements. This approach allows the hysteretic law of the different subelements to be simpler and, thus, more general than previous elements, while the member still exhibits a complex hysteretic behavior.

In conclusion, member models have some advantages and disadvantages. The advantages are:

1. simplicity of formulation and relatively low computational cost;
2. calibration of the model by trial and error or more formal system identification methods is often easy, because of available experimental data in the form of moment-rotation relations;
3. the implementation of these models in existing nonlinear dynamic analysis programs is relatively straightforward;
4. the results can easily be represented in a form that is directly useful to designers.

The disadvantages of member models are as follows:

1. These models are, without exception, phenomenological models of member behavior, which cannot be easily extended to general loading conditions. For example, most models to date only approximate the effect of gravity loads. The interaction between bending moment, shear and axial force is described by empirical hysteretic rules, which can quickly become extremely complex and are often valid only for the few cases, for which they were calibrated.
2. The parameters of these models cannot be readily established in many cases. This is particularly true for concentrated plasticity models. A few attempts at establishing general rules for the derivation of model parameters are limited to the simplest cases, e.g. beam elements without shear and axial force.
3. The definition of damage is often rather arbitrary in these models. One is limited to overall measures of damage, such as rotations, instead of the more rational local measure of strain in certain regions of the member.

b) Fiber Models

In fiber models, a member is subdivided longitudinally into a number of segments, and these are, in turn, subdivided into a number of steel and concrete fibers. The member behavior is then derived by postulating the stress-strain behavior of these fibers and integrating over the cross section to obtain the moment-curvature relation, which is, in turn, integrated along the member to yield the moment-rotation relation. This process can be formally summarized:

The element force resultants and the corresponding deformations are:

$$\mathbf{Q} = \begin{Bmatrix} M_1 \\ M_2 \end{Bmatrix} \quad \mathbf{q} = \begin{Bmatrix} \theta_1 \\ \theta_2 \end{Bmatrix} \tag{6-12}$$

The deformation field is the curvature distribution $\chi(x)$ along the element. The corresponding action field is the moment distribution $M(x)$. Following the *stiffness approach*, three major steps are performed:

1) *Compatibility:* the element deformation field is expressed as a function of the element deformations $\mathbf{q}$,

$$\chi(x) = \mathbf{a}(x)\mathbf{q} \tag{6-13}$$

2) *Constitutive Law:* the relation between section deformation $\chi(x)$ and section moment $M(x)$ can be written as

$$M(x) = g(\chi(x)) \tag{6-14}$$

This linearization introduces an approximation error which is normally corrected through an iteration scheme. A moment-curvature relation at each section is either derived by summing up over all section fibers or it is postulated as a material law. The former approach is more time consuming, but more general. This relation can be linearized as follows,

$$M(x) = k(x)\chi(x) \tag{6-15}$$

where $k(x)$ is the section stiffness.

3) *Equilibrium* is imposed by applying the principle of virtual displacements,

$$\int_0^L \delta\chi(x)M(x)dx = \delta\mathbf{q}^T\mathbf{P} \tag{6-16}$$

$$\delta\mathbf{q}^T\left[\int_0^L \mathbf{a}(x)^T k(x)\mathbf{a}(x)dx\right]\mathbf{q} = \delta\mathbf{q}^T\mathbf{P} \tag{6-17}$$

$$\mathbf{K}\mathbf{q} = \mathbf{P} \tag{6-18}$$

where

$$\mathbf{K} = \int_0^L \mathbf{a}(x)^T k(x)\mathbf{a}(x)dx \tag{6-19}$$

is the element stiffness matrix and $\mathbf{P}$ the vector of the externally applied loads.

A problem with fiber models is the selection of shape functions for member deformations $a(x)$. The stiffness approach, which is outlined above, satisfies equilibrium along the member in a weighted or average way. This often leads to

numerical problems under cyclic load reversals, as has been well demonstrated in a paper by Zeris and Mahin (1988). The problem can be remedied by deriving the element stiffness matrix **K** using the flexibility approach. In this case equilibrium along the member is satisfied exactly at all times. Unfortunately, the solution proposed by Zeris and Mahin does not guarantee that compatibility is satisfied along the element, and this can also lead to numerical problems. So far, no clear solution to the problem has been proposed, but it appears that a flexibility formulation based on an event-to-event solution strategy can be successful.

An interesting variation of the types of models mentioned above is the multi-spring model proposed by Li, Otani, and Aoyama (1988) and Zhou et al (1990). Well suited for columns subjected to biaxial bending plus axial forces, this model can simulate member behavior with a set of calibrated nonlinear springs and can be considered an extension of fiber and plastic hinge models.

In conclusion, the advantages of fiber models are:

1. These models are rational in the sense that the element behavior is derived from the fundamental stress-strain relation of the constituent materials. Thus they can model in a direct way the effect of detailing on the member behavior (e.g effect of longitudinal and transverse reinforcement distribution). They can also account for the interaction between axial force and bending moment in a very straightforward way, without modification of the initial formulation of the model. To date, however, no fiber model has been proposed which accounts for the effect of shear and bond-slip of reinforcing steel. These effects are very important in the seismic response of reinforced concrete structures, particularly, short columns or piers.
2. As is the case with member models, the results of fiber models are in a form that is directly useful to designers.
3. Damage can be directly related to the strains experienced by the fibers. This allows for the formulation of rational damage models. Calibration of such models is, however, more difficult than in the case of member models.

The disadvantages of fiber models are:

1. To be able to realistically trace the hysteretic behavior of RC members, a large number of fibers is needed. This leads to high computational costs, which preclude the use of such models in the dynamic response analysis of large structures. A way to overcome this problem is to use fiber models as a front end for the calibration of simpler models. These simpler models can either be fiber models with a very small number of fibers or member models such as those described in the preceding section.
2. The calibration of fiber models against available experimental data is not as straightforward as that of member models, because of the larger number of parameters. At the same time, however, calibrations performed on a number of specimens should be much more ready to be extended to other cases than is the case for member models.

c) Hysteretic Models

To describe the hysteretic behavior of the nonlinear springs at the ends of the one-component model a hysteretic law is needed. The first such law was proposed by Clough (1966). A more refined hysteresis model was proposed by Takeda et al. (1970), in which the monotonic behavior is described by a trilinear skeleton curve that accounts for cracking of concrete and yielding of

reinforcing steel. The hysteretic behavior is described through a number of rules for unloading and reloading that were derived from specimens tested on an earthquake simulator. Even though Takeda's model was originally proposed for simulating the load-displacement relation of RC subassemblages, it has been widely used since for the description of both hysteretic moment-curvature and moment-rotation relations of RC members.

Anderson and Townsend (1977) investigated the effect of different hysteretic models on the dynamic response of RC frames. Four different models were used to describe the hysteretic behavior of critical regions of RC members: (a) a bilinear elastic-strain hardening model, (b) a bilinear degrading model with equal unloading and reloading stiffness, (c) a trilinear degrading model with different stiffness for unloading and reloading and (d) a degrading trilinear model for beam-column connections. They studied the effect of reinforcing bar slippage in the joint by inserting a small hinge element of predefined length between the rigid joint element and the flexible girder element. The study shows that the reduction in stiffness of reinforced concrete elements due to inelastic deformations can have a significant effect on the dynamic response of frame structures. Among the different hysteretic models used in the study the degrading trilinear connection model appears to be the most accurate. It is also shown that the use of a degrading stiffness model results in an increase in interstory displacements. This can have a significant effect on the load carrying capacity of the structure due to the $P - \Delta$ effect arising from high axial forces.

The effect of different hysteresis models on the nonlinear dynamic response of a simple concrete specimen was studied by Saiidi (1982). He analyzed four models: elastic-perfectly plastic, elasto-plastic with strain hardening, Clough's model and a new Q-hysteresis model. The first two are very simple, but quite unrealistic models of reinforced concrete; the other two are more accurate and differ mainly in the representation of stiffness degradation during unloading and reloading. The performance of the different hysteretic models was evaluated by comparing the results with those obtained using Takeda's model, since its agreement with a large number of experimental data is excellent. Poor agreement with Takeda's model is exhibited by both elasto-plastic models; Clough's model shows relatively good agreement and the Q-hysteresis model shows excellent agreement. The study concludes that stiffness degradation effects during unloading and reloading are very important in determining the overall response of RC structures, because they affect the amount of energy dissipated by the structure.

d) Bond-Slip and Shear Effects

The member models of the preceding sections do not include the effect of shear and bond-slip in an explicit way, except for the modification of the hysteretic models. This is at best a very approximate way and lacks generality, since the hysteretic models cannot be easily extended to cases, which have not been used in the initial calibration of the model.

A more rational way to include the effects of shear and bond-slip in member models is to address these effects explicitly in member and fiber models. Only few studies are known to date in this direction. Filippou and Issa (1988) have proposed to subdivide the member into a number of subelements, with each subelement modeling one effect (e.g. shear or pull-out from beam-column joint),

using its distinct hysteretic rule. Naturally, the most rational way to include these effects is by means of microscopic finite element models. No studies exist in which shear and bond-slip effects were incorporated into fiber or layer models.

A few studies have been conducted since the early 1980's to model the bond-slip behavior of single reinforcing bar anchorages and reinforcing bars anchored in beam-column joints. The first group of models makes use of the finite difference method in the solution of the differential equations of bond (Viwathanatepa et al. 1979; Tassios and Yannopoulos 1981; Ciampi et al. 1982; Filippou et al. 1983a,b; Hawkins et al. 1987).

The second group of models solves the bond problem by assuming a parabolic or exponential function for the bond stress along the anchorage length of the reinforcing bars. Filippou (1986) used a piecewise linear bond stress distribution, which is established iteratively by satisfying the equilibrium and compatibility conditions of the bond problem.

In the third group of models the differential equations of bond are solved in closed form. The model proposed by Harajli et al. (1988) uses this approach to predict the distribution of relative slip, bond stress and steel stress along reinforcing bars anchored in interior beam-column joints. The model makes use of the monotonic bond stress-slip relation in confined concrete and only indirectly accounts for bond deterioration under cyclic load reversals. This fact limits its applicability to slip reversals of moderate magnitude. A closed form series solution is proposed by Russo et al. (1990) for the differential equations of bond, based on a bilinear steel model and the local bond stress-slip relation proposed by Eligehausen (1983). The advantage of this solution approach is that no iterations are required. Since the study is only limited to the portion of the reinforcing bars which is surrounded by the confined concrete of the joint core, it is unclear whether the model can be extended to account for the extensive bond damage which takes place in unconfined concrete regions under cyclic load reversals.

During the last fifteen years several hysteretic models of beam-column joint behavior were proposed. A number of these were also used in nonlinear earthquake response analysis of structures. These models, generally, fall in three categories.

The first group consists of models which are derived from experiments on full or reduced scale beam-column joint subassemblages subjected to cyclic excitations (Townsend and Hanson 1972; Soleimani et al. 1979; Anderson and Townsend 1977). These models agree well with the experiments they were derived from, but generalization to different configurations and other loading conditions is somewhat doubtful, because model parameters were selected to fit the particular experimental results and not from physical interpretation of the mechanisms which contribute to the observed behavior.

The second group of joint models is derived in connection with analytical studies. These models are, typically, composed of a bilinear or trilinear monotonic envelope curve and an associated set of rules which define the hysteretic behavior under cyclic load reversals (Otani 1974; Emori and Schnobrich 1981; Banon et al. 1981).

The third group of joint models is based on finite element idealizations. Noguchi (1981) has developed a finite element model for the nonlinear analysis of reinforced concrete beam-column joints under monotonic loading with emphasis on the different bond characteristics along the reinforcing bars passing through the joint. In this model a simplified bilinear model describes the steel stress-strain relation, and an equivalent uniaxial stress-strain curve describes the concrete behavior in compression. Bond is modeled by a link element with an idealized bond stress-slip relation. The crack pattern and location is fixed before the start of the analysis and a crack link element connects two nodes, one on each face of the crack. The predictions of the model agree fairly well with experimental results. Later, Noguchi et al. (1984a,b) extended the model to beam-column joints under cyclic load reversals, paying particular attention to the constitutive relation of concrete, the opening and closing of the cracks and the cyclic bond stress-slip relation. The results of these studies indicate that the stiffness deterioration of the subassemblage is influenced by the failure of concrete in shear and by bond deterioration along the reinforcing bars in the joint.

Filippou et al. (1983a,b) have developed a model of the hysteretic behavior of reinforced concrete beam-column joints which is also based on the finite element method. This model accounts for the cyclic bond deterioration along the anchored bars and the associated relative slippage between bars and surrounding concrete. The slippage of the reinforcing bars in the joint leads to an interaction between the forces acting at the two beam-column interfaces of an interior joint. These forces are determined from a new hysteretic model for cracked reinforced concrete sections. The proposed joint model describes quite well the hysteretic behavior of beam-column joints under generalized excitations but does not include the effect of shear.

In 1987 Noguchi et al. used the finite element method to describe the shear resistance of reinforced concrete beam-column joints under cyclic load reversals. Tada (1987) has also proposed a finite element model of the beam-column joint and the adjacent girder inelastic regions, which takes into account the bond deterioration along the anchored bars under cyclic load reversals.

## 6.5 Dynamic Analysis Aspects

### 6.5.1 Time-Discretization in Structural Dynamics

The equations of motion of a structure are well known,

$$\mathbf{M}\ddot{\mathbf{u}} + \mathbf{C}\dot{\mathbf{u}} + \mathbf{K}\mathbf{u} = \mathbf{f}, \qquad (6-20)$$

where $\mathbf{u}$ is the vector containing the displacement and rotational degrees of freedom of the discretized structure; $\mathbf{M}$, $\mathbf{C}$ and $\mathbf{K}$ are the mass, damping, and stiffness matrices, respectively; the right-hand side vector $\mathbf{f}$ contains the external loads acting on the structure.

The key issue of structural dynamics is to integrate Eq. 6-20 as accurately and as economically as possible at the same time. The accuracy and economy of the various methods that are available depend strongly upon the type of problem at hand. The major factor that determines which method is most suitable for a

certain problem is the loading rate. As a rule of thumb, one might say that wave propagation problems, which typically arise from blast and impact loadings with high strain rates, are more conveniently analyzed using *explicit* time integrators. *Implicit* time integrators have their merit for analyzing problems that involve lower strain rates, e.g., problems involving earthquake or wind loadings. In the latter class of problems a much larger time span has to be analyzed. The limited time step size needed in explicit methods renders these uneconomical, because it would simply involve far too many time steps.

In the sequel we will first give examples of explicit and implicit time integrators such as the popular central difference and Newmark schemes. For both classes of methods we will comment on their stability and accuracy properties. Further, some comments will be made on issues like nonlinear material behavior and implicit-explicit time integration methods.

A popular prototype of explicit time integrators is the central difference method, which approximates the nodal accelerations and velocities at time $t$ by the finite difference approximations,

$$\ddot{u}^t = \frac{1}{\Delta t^2}[u^{t-\Delta t} - 2u^t + u^{t+\Delta t}] \qquad (6-21)$$

and

$$\dot{u}^t = \frac{1}{2\Delta t}[-u^{t-\Delta t} + u^{t+\Delta t}] \qquad (6-22)$$

respectively, with $\Delta t$ being the time interval considered. Substitution of these expressions into the equations of motion, Eq. 6-20, at time $t$,

$$\mathbf{M}\ddot{\mathbf{u}}^t + \mathbf{C}\dot{\mathbf{u}}^t + \mathbf{K}\mathbf{u}^t = \mathbf{f}^t, \qquad (6-23)$$

yields the following expressions for the nodal displacements at time $t + \Delta t$,

$$\left(\frac{1}{\Delta t^2}\mathbf{M} + \frac{1}{2\Delta t}\mathbf{C}\right)\mathbf{u}^{t+\Delta t} = \mathbf{f}^t - \left(\mathbf{K} - \frac{2}{\Delta t^2}\mathbf{M}\right)\mathbf{u}^t - \left(\frac{1}{\Delta t^2}\mathbf{M} - \frac{1}{2\Delta t}\mathbf{C}\right)\mathbf{u}^{t-\Delta t}. \qquad (6-24)$$

It is apparent that Eq. 6-24 can be solved directly for $\mathbf{u}^{t+\Delta t}$, since $\mathbf{u}^{t-\Delta t}$ and $\mathbf{u}^t$ are known. It is for this reason that the method is called explicit. When the time step is kept constant, the matrix on the left-hand side of the equation needs to be factorized only once, and the whole process is reduced to a sequence of forward and backward substitutions, thus greatly reducing the computational effort involved. This effort is reduced even further, if the mass and damping matrices are diagonal. For the mass matrix, this implies that some lumping scheme is applied, so that the method is particularly effective for low-order finite elements. The equation system becomes effectively uncoupled, which has major advantages for parallel and vector processing. Indeed, very efficient because highly vectorizable codes can be written, when the above-described approach is adopted. Examples are the NIKE and PRONTO codes for analyzing impact phenomena.

A disadvantage of explicit methods such as the central difference method is their conditional stability, which implies that the scheme is only stable when the time step is smaller than a certain threshold value. For time steps larger than this critical value, errors in the boundary conditions, round-off errors, etc. will be amplified and will dominate the response after a sufficient number of time steps, thus rendering the solution meaningless. Depending on the mesh layout, this restriction on the time step may be quite severe.

To overcome the problem of having to use very small time steps, especially for problems that do not involve high loading rates, implicit time integrators have been developed, which allow time steps that are orders of magnitude larger than the critical time step for explicit integrators. One of the most popular classes of time integrators is the Newmark family. Its main assumption is that the acceleration varies linearly over the time step, so that,

$$\dot{u}^{t+\Delta t} = \dot{u}^t + \Delta t[(1-\gamma)\ddot{u}^t + \gamma\ddot{u}^{t+\Delta t}] \qquad (6-25)$$

and

$$u^{t+\Delta t} = u^t + \Delta t\dot{u}^t + \frac{1}{2}\Delta t^2[(1-2\beta)\ddot{u}^t + 2\beta\ddot{u}^{t+\Delta t}]. \qquad (6-26)$$

In contrast to the central difference scheme, where the equations of motion are satisfied at time $t$, the Eqs. 6-25 and 6-26 are substituted into the equations of motion at time $t+\Delta t$,

$$\mathbf{M}\ddot{\mathbf{u}}^{t+\Delta t} + \mathbf{C}\dot{\mathbf{u}}^{t+\Delta t} + \mathbf{K}\mathbf{u}^{t+\Delta t} = \mathbf{f}^{t+\Delta t}, \qquad (6-27)$$

with the result,

$$\tilde{\mathbf{K}}\mathbf{u}^{t+\Delta t} = \tilde{\mathbf{f}}^{t+\Delta t}, \qquad (6-28)$$

where

$$\tilde{\mathbf{K}} = \mathbf{K} + a_o\mathbf{M} + a_1\mathbf{C} \qquad (6-29)$$

$$\tilde{\mathbf{f}} = \mathbf{f} + \mathbf{M}(a_o\mathbf{u}^t + a_2\dot{\mathbf{u}}^t + a_3\ddot{\mathbf{u}}^t) + \mathbf{C}(a_1\mathbf{u}^t + a_4\dot{\mathbf{u}}^t + a_5\ddot{\mathbf{u}}^t), \qquad (6-30)$$

and the coefficients $a_0, \ldots, a_5$ are given by

$$a_o = \frac{1}{\beta\Delta t^2}, \quad a_1 = \frac{\gamma}{\beta\Delta t}, \quad a_2 = \frac{1}{\beta\Delta t}, \qquad (6-31)$$

$$a_3 = \frac{1}{2\beta} - 1, \quad a_4 = \frac{\gamma}{\beta} - 1, \quad a_5 = \frac{1}{2}\Delta t(\frac{\gamma}{\beta} - 2). \qquad (6-32)$$

By changing the values of the free parameters $\beta$ and $\gamma$, a whole range of time integration methods is obtained. For instance, for $\beta = 0$ and $\gamma = \frac{1}{2}$, the (explicit) central difference scheme is retrieved. In fact, the Newmark family contains a whole set of explicit time integrators, since for $\beta = 0$, the stiffness matrix $\mathbf{K}$ disappears from the modified stiffness matrix $\tilde{\mathbf{K}}$.

It is important to note that even the members of the Newmark family, that are implicit in nature, are not necessarily unconditionally stable. It can be proven (e.g. Bathe 1982; Hughes 1983; Hughes 1987; Geradin, Hogge and

Roberts 1987), that unconditional stability for the Newmark family is assured only if

$$\gamma \geq \frac{1}{2} \quad \text{and} \quad \beta \geq \frac{1}{4}(\gamma + \frac{1}{2})^2.$$

A most prominent member of the Newmark family that satisfies the above requirement is the constant, or average, acceleration method, which is obtained by setting $\beta = \frac{1}{4}$ and $\gamma = \frac{1}{2}$. Alternatively, this method may be thought of as a trapezoidal rule.

Although a stable algorithm ensures that errors are not amplified in the course of time, the errors themselves can be quite large. In other words, stability does not necessarily imply accuracy of the time integrator. Generally, this is only the case for conditionally stable time integrators, for which the limitation imposed on the time step by the stability requirement nearly always warrants sufficient accuracy. For unconditionally stable time integrators, a rule of thumb is that the time step should be chosen smaller than the time that the wave needs to reach the next nodal point in the finite element mesh. If the wave velocity is $c$ and the distance between two nodes is $L$, the time step size should satisfy the condition,

$$\Delta t \leq \frac{L}{c}. \qquad (6-33)$$

The notions of stability and accuracy have been introduced here in a rather intuitive fashion. More precise treatments can be found in (Bathe 1982; Hughes 1983; Hughes 1987; Geradin, Hogge and Roberts 1987).

Implicit methods can be categorized into one-step methods such as Newmark's algorithm and so-called linear multi-step (LMS) algorithms. A method that belongs to the latter class and seems to be attractive for nonlinear dynamic analyses of concrete structures is the Hilber-Hughes-Taylor $\alpha$-method (Hughes 1983; Hughes 1987; Geradin, Hogge and Roberts 1987). It retains the approximations for the velocity and the displacement at time $t + \Delta t$, as defined in Newmark's scheme (Eqs. 6 and 7), but the equation of motion at time $t + \Delta t$ is replaced by

$$\mathbf{M}\ddot{\mathbf{u}}^{t+\Delta t} + (1+\alpha)\mathbf{C}\dot{\mathbf{u}}^{t+\Delta t} - \alpha\mathbf{C}\dot{\mathbf{u}}^{t} + (1+\alpha)\mathbf{K}\mathbf{u}^{t+\Delta t} - \alpha\mathbf{K}\mathbf{u}^{t} = (1+\alpha)\mathbf{f}^{t+\Delta t} - \alpha\mathbf{f}^{t}. \qquad (6-34)$$

For $-\frac{1}{3} \leq \alpha \leq 0$, $\gamma = \frac{1}{2}(1-2\alpha)$ and $\beta = \frac{1}{4}(1-\alpha)^2$, the method is unconditionally stable. The $\alpha$-method can be viewed as a logical extension of the Newmark method with improved characteristics for nonlinear problems. Successful applications of this method to dynamic loading of concrete structures have been reported by Glemberg (Glemberg 1984). A disadvantage of LMS-methods is that, unlike one-step methods, they require special treatment for starting up the process.

Another important issue in dynamic analysis of nonlinear structural behavior is, that within each time step, equilibrium iterations must be carried out to maintain sufficient accuracy. This holds even if the time step is selected in line with the above recommendations. The reason is that the inherent path-dependency of concrete behavior (cracking, crushing, etc) causes errors, which else will be dragged along to subsequent times. Either a Newton-Raphson scheme, usually in a modified form, in which the stiffness matrix is updated only

once in each time step, or quasi-Newton update methods can be employed for this purpose.

A final important evolution of the past decade is the development of implicit-explicit integration methods (e.g., Hughes 1983; Park and Felippa 1983). Sometimes assemblies have to be analyzed, which consist of a relatively stiff and a relatively soft part. Examples are soil-structure interaction and fluid-structure interaction problems. Analyzing the soft subassembly with the same integrator and the same time step as the stiff subassembly may be uneconomical. Indeed, it may prove versatile to employ an explicit time integrator for the soft assembly, e.g. the fluid, while an implicit, unconditionally stable algorithm is used for the stiff subassembly, e.g. the structure. The rationale is that the critical time step for an explicit method in the soft part may be many times larger than the critical time step in the stiff part. In addition to using different kinds of time integrators for these different parts, different time step sizes may be used to further improve efficiency.

### 6.5.2 Use of Crack Models in Structural Dynamics

Since one of the major sources of nonlinear behavior of concrete structures is cracking, it is important to examine the consequences thereof in dynamic analysis. The capacity to transmit tensile forces obviously decreases after cracking. This can be drastic in the sense of an immediate stress drop to zero (perfectly brittle behavior), or gradual when a tension-softening model is employed. In either case, a severe dependence on the element size is found. Although in the sequel the attention is focussed on softening models, the observations and conclusions pertain equally to brittle cracking.

Recent studies (Belytschko and Bazant 1984; Read and Hegemier 1984; Sandler 1984) on the validity of strain-softening models in dynamic analyses of concrete structures have shown that strain softening causes stability problems and pathological mesh sensitivity. Sandler (1984) has shown analytically for a simple problem, a one-dimensional rod with prescribed velocity, that a small change in the load results in large differences in the response. Bazant and Belytschko (1985), Belytschko and Bazant (1984) and Sandler (1984) also noted an excessive dependence of the solution on the mesh in the sense that failure always occurred in one or two rows of elements. Since in classical continuum models the energy dissipation depends on the size of the elements, this implies that the structure can fail without energy dissipation.

The problem of mesh sensitivity under dynamic loading conditions can be demonstrated analytically for one-dimensional problems. Then the governing equations can be formulated as

$$\sigma_{,x} = \rho u_{,tt} \qquad (6-35)$$

$$\sigma_{,t} = E(\epsilon)\epsilon_{,t} \qquad (6-36)$$

$$\epsilon = u_{,x} \qquad (6-37)$$

$\rho$ is the density and $E$ is the tangent modulus which depends on the strain $\epsilon$. The commas denote partial differentiation. Eqs. 6-35 to 6-37 can be combined to give the standard one-dimensional wave equation,

$$u_{,xx} = \frac{1}{c^2} u_{,tt} \qquad (6-38)$$

with

$$c^2 = \frac{E(\epsilon)}{\rho} \qquad (6-39)$$

the longitudinal wave velocity. When the strain softening regime is entered the tangent modulus $E(\epsilon)$ becomes negative. As a consequence, the system of equations changes from a hyperbolic system into an elliptic system. The initial value problem becomes ill-posed.

Bazant and Belytschko (1985) have shown analytically that the occurrence of strain softening produces a strain which immediately localizes and becomes infinite within a time interval that approaches zero. The stress in the strain-softening section drops to zero instantly, and the deformation is limited to a point as soon as strain softening occurs. The consequence is that the structure can fail without energy dissipation.

Another peculiarity is that the edge between the softening and the elastic sections becomes an internal boundary. Waves reflect on this internal boundary in the same way as on a free boundary: tensile waves reflect as pressure waves and vice versa. Accordingly, when a section of a bar enters the softening regime, it is no longer possible to transmit data between points at both sides of the softened zone.

The abovementioned problems are also encountered in numerical computations of cracking in concrete. It is found that different meshes produce significantly different results, wherein the degree of localization depends completely on the spacing of the mesh. Inelastic deformation invariably localizes in a single element which is attended by high strain rates. For an infinite number of elements the strain rate even becomes infinite.

In the next paragraphs, some examples will be given to illustrate the pathological mesh sensitivity, when strain softening is introduced in the constitutive equations.

A one-dimensional bar is subjected to an impact tensile load. The load is present in a short time interval, which is smaller than the first eigenperiod. The wave speed $c$ is 3227 m/sec, and the duration of the impact load is $7.75 \cdot 10^{-4}$ *sec*, so that the wavelength is 2.5 m.

Two calculations are considered, one in which the bar was divided into five eight-noded elements, and one in which the bar was divided into ten eight-noded elements. Nine-point Gauss integration has been employed throughout the analysis to avoid the occurrence of spurious mechanisms (de Borst and Rots 1989). For other data the reader is referred to Sluys (1989a).

The magnitude of the impact load is taken as 65% of the maximum tensile load in the static case. The response of the bar is linear elastic until the left boundary is reached. There the wave reflects as a tensile wave, which causes a locally higher stress and results in cracking. The material starts to soften, and strain localization takes place. A small drop in the stress and a rapid increase of the strain can be observed. During loading the width of the localization band is constant until the tensile wave has passed.

Using 40 elements, the ultimate crack strain is much higher than in the calculation with the ten-element mesh. In Fig. 6.8, the strain distribution along the bar at maximum strain has been plotted for both meshes. In both analyses localization remains limited to one vertical row of integration points.

The stress drop converts the boundary into a free one, and the tensile wave is almost totally reflected as a pressure wave. This can be seen from the energy consumption in the system in Fig. 6.9. In the remaining system the wave propagates through a bar with two free ends, alternately as a pressure and as a tensile wave. When a pure brittle crack model is used, the results become even worse (Sluys 1989a).

It is finally noted that the above results were obtained in spite of the fact that a $G_f$-type model was employed to ensure a mesh-objective energy release. It appears that in contrast to the static case, where the global behavior can be made insensitive to mesh-refinement by using a $G_f$-type model, or in other words by making the softening modulus dependent on the element size, this is not the case for dynamic loadings. This is because the extent of wave reflections depends on the locally occurring stress-strain condition, which changes when the mesh is refined. Recently, some fresh approaches have been put forward to remedy this pathological behavior. Among these, methods which set out to enrich the continuum description by adding rotations as independent degrees of freedom (Sluys and de Borst 1990a,b), or by making the stress in the softening regime a function not only of the strain but also of higher-order derivatives thereof (Schreyer and Chen 1986; Lasry and Belytschko 1988), or by adding strain-rate sensitivity to the system (Needleman 1988; Sluys and de Borst 1990a) seem to be most promising for large-scale computations, although the developments in this field are so fast that firm statements cannot be made on this issue.

### 6.5.3 Numerical Simulation of Uniaxial Impact Tests

In the Stevin Laboratory of Delft University of Technology, uniaxial tensile impact tests have been carried out on notched, prismatic concrete specimens. A geometry with notches makes it possible to fix the failure plane and to measure the deformation inside as well as outside the fracture zone. The tests have been performed with the Split-Hopkinson bar apparatus by Weerheijm and Reinhardt (1989), Fig. 6.10. The specimen is kept between an upper and a lower bar, and the pulse is applied at the bottom of the experimental set-up. The loading rate has been measured after the pulse passed the specimen and has been affected by the failure process and the geometry of the specimen.

Numerical analysis of the uniaxial tensile impact tests have been carried out in order to demonstrate the mesh-sensitive behavior and the influence of the structural response on the load-displacement data (Sluys 1989b, Sluys and de Borst 1990b). In the numerical analysis three restrictions have been made. First, the analysis has been performed under the assumption of plane stress, while in the experiment three-dimensional effects may have played a role. Secondly, the numerical model for the experimental set-up differs from the one actually used. Because the boundary conditions may influence the response, this assumption in modelling should be investigated. Thirdly, the material was modelled as rate-independent, whereas rate effects may have a major influence on the material properties.

In all numerical analyses, use has been made of the implicit Newmark integration scheme, with coefficients $\beta = \frac{1}{4}$ and $\dot{\gamma} = \frac{1}{2}$. The time step was taken as $2 \cdot 10^{-6}$ *sec* to achieve an adequate description of the failure process. If we assume that the loading wave traverses at the most one element in a time step, a maximum element size can be derived. Using this element size, the total Split-Hopkinson bar with a height of 11.2 m should be modelled with approximately 4000 elements to accurately simulate a propagating loading wave through the set-up. This would make a dynamic nonlinear analysis too expensive. Instead, an investigation has been carried out for a configuration with less elements using special boundary elements to slow down the loading wave without undesirable reflections. A detailed description of the numerical modelling of the Split-Hopkinson bar has been given by Sluys (1989b). For the specimen itself, two finite element discretizations have been used, Fig. 6.11. First, a fine mesh consisting of quadrilateral elements with eight nodes and a four-point Gauss integration, and triangular elements with six nodes and a three-point Gauss integration has been used. The reduced cross section has been modelled with two rows of elements. The second mesh was coarser, with only one row of elements in the notched section. Here, only quadrilateral elements with eight nodes and nine-point Gauss integration have been used.

In the calculations, one element in front of the left-hand notch was given a material imperfection in the sense that the tensile strength has been reduced by 20%. When such an imperfection is not inserted in the model, a symmetric deformation and failure pattern will be computed. Because of the heterogeneous character of concrete, imperfections will always exist, and the asymmetric solution is observed in static (Reinhardt et al. 1986) as well as in dynamic experiments (Weerheijm and Reinhardt 1989).

The computational results for the fine mesh show deformation and cracking behavior which is in contradiction with the experimental data. Cracks start propagating from both sides of the specimen in two different rows of elements. Convergence problems occur when vertical cracks appear among the two rows of elements. It appeared that when a conventional softening model is used, numerical results can only be made in accordance with experimental data when the element size in the fracture zone approximately equals the crack band width (the coarse mesh of Fig. 6.11).

In the first analysis with the coarse mesh the material properties have been derived directly from the tests: $E_c = 33863\ N/mm^2$, $f_{ct} = 4.22\ N/mm^2$ and $G_f = 100\ J/m^2$. Now, asymmetric crack propagation occurs similar to the test, Fig. 6.12. However, in the experiment, the failure mode was dominated by rotation, whereas the calculated failure mode was dominated by translation, and only a small rotation of the specimen can be observed. In Fig. 6.13, the stress-deformation curve for the fracture zone has been plotted, in which $u$ represents the deformation inside the fracture zone, and $\sigma_{yy}$ represents the vertical stress at the top of the specimen. The numerical analysis shows a behavior which is far more ductile after peak stress than is observed experimentally. The maximum stress differs considerably from the measured value in the test, which is due to the presence of stress concentrations adjacent to the notches. To achieve a more pronounced rotation failure mode and a more brittle behavior after peak stress, a purely brittle softening model has been used next. This model is the limiting case wherein the stress drops to zero instantly upon crack initiation.

The results, Fig. 6.13, show that as soon as cracking starts, the stress hardly increases, which is due to the inability of the cross section to redistribute stresses. The specimen rotates slightly, but the results for the tensile strength are totally unrealistic. Finally, a modified analysis has been carried out with an increased tensile strength, $f_{ct} = 5.6\ N/mm^2$ and a decreased value for the fracture energy, $G_f = 60\ J/m^2$. The results improved with respect to the peak stress but still show less rotation and ductile behavior after peak stress, Fig. 6.11. So it becomes clear that by using a conventional strain-softening model, a modification of the input parameters improves the situation, but it is impossible to properly simulate the failure mechanism of the specimen. After the appearance of cracks, there exists an obvious difference between experiment and simulation with respect to the stiffness of the specimen. More energy should be dissipated between crack initiation and peak stress to achieve larger deformations, which corresponds to a more ductile softening function. On the other hand, after peak stress a more brittle model is exactly what is needed to describe the post-peak behavior more accurately.

In sum, due to the mesh sensitivity, the numerical analysis only gives reasonable results when the element size equals approximately the crack band width observed in the test. The material parameters derived directly from the test are influenced by the structural response and better results can be obtained by a modification of these parameters. However, the failure mechanism observed in the test is difficult to describe with a conventional softening model.

## 6.6 Practical Applications and Examples

### 6.6.1 General

The application of nonlinear dynamic finite element analysis to realistic reinforced concrete structures requires considerable expense and exemplary skills on the part of the analyst. These two factors are likely to inhibit the routine use of this analysis tool in engineering practice for some time to come. Yet, there are situations, in which the problem facing the engineer cannot be solved any other way, short of full-scale experimentation. Even scale model tests are difficult to dvise, if all dynamic properties are to be scaled properly.

The examples given below shall serve to illustrate both the potential and the difficulties of nonlinear finite element analysis.

### 6.6.2 Internal Gas Explosion in an Underwater Tunnel

In an effort to demonstrate the applicability of nonlinear finite element analysis to problems in engineering practice in general, and to highlight the capabilities of the general finite element program DIANA (de Borst et al. 1983) in particular, the Dutch Committee for Research, Codes and Standards for Concrete (CUR-VB) has funded a project that has since been documented in the so-called DIANA-example book (van Mier 1987). The example to be described below is the last of the eight examples contained in that report.

Road tunnels that pass under waterways are very common in the Netherlands. They are normally designed to resist the loads associated with soil and water pressure. In the event of an internal gas explosion, the tunnel experiences

a load reversal for which it may not be adequately reinforced. Thus, the question whether hazardous cargo should be permitted to pass through such tunnels is of some importance. Fig. 6.14 shows a cross section and material properties typical for such tunnels. The strength parameters listed in Fig. 6.14 are based on experimentally determined values, with a 20% allowance for the strain-rate effect.

It was the objective of the analysis to predict the response of the tunnel to the pressure load associated with a hypothetical internal gas explosion. The assumed pressure time history is indicated in Fig. 6.15.

The solution of a problem of this nature requires a careful step-by-step approach, with continuous verification of the correctness of the program, the finite element model, and the results obtained. In order to achieve these goals, the following analyses were performed:

1. a linear elastic static frame analysis of the entire tunnel cross section;
2. a linear static finite element analysis of a segment of the tunnel roof;
3. a nonlinear static finite element analysis of the same tunnel roof segment;
4. an eigenvalue analysis of the finite element model;
5. a nonlinear dynamic time history analysis of a grossly simplified finite element model;
6. the final nonlinear dynamic time history analysis of the actual finite element model.

At each step, measures were taken to verify that the analysis results were reasonable. For this purpose it was very helpful that a 1:5 scale model of a particular tunnel section had been tested earlier. Only selected results of analysis steps 3 and 6 will be shown here. Further details may be found in (van Mier 1987; Meyer 1987b). Figure 16 shows the finite element model, which represents a segment of the tunnel roof, making use of symmetry. 45 eight-noded plane stress elements represent the concrete, and the reinforcement was modeled by 34 bar elements, resulting in a total of 172 nodes with 344 potential degrees of freedom. When comparing the results of a nonlinear static analysis of this model with the response recorded on the scale model in the experiment, Fig. 6.17, a considerable discrepancy is apparent. Several reasons could be identified to explain this difference in a qualitative sense. In the experiment, load was increased in stages, and each load level (except for the final one) was applied 10,000 times. The static analysis assumed monotonic load application and therefore did not capture the damage that accumulated during the large number of load cycles. It also did not include the creep deformations that took place during the experiment. Finally, concrete cracking can be expected to cause some moment redistribution and thus affect the boundary conditions for the finite element model, which were held constant throughout the analysis.

Even though the analysis overestimated the stiffness of the structure, cracking patterns were reproduced rather accurately, and also the failure mode and failure load level agreed remarkably well, Fig. 6.17. It was primarily this encouraging agreement which gave rise to the confidence that it was possible to use DIANA to compute the tunnel reponse up to failure.

The final nonlinear dynamic analysis consisted of 150 time steps of 1.25 msec step size. The acceleration, velocity, and displacement time histories of the roof midspan section are shown in Fig. 6.18. The first impact experienced

by the structure was the axial load at the left boundary as a result of the pressure on the vertical tunnel walls. This tensile impact wave propagated to the right at about 737 m/sec, causing largescale concrete cracking in its wake and reaching the right boundary (roof midspan) after only seven time steps, long before the roof had any time to respond in bending to the upward pressure, Fig. 6.19. This "concrete cracking wave" was followed by a slower "steel yield wave", which caused the first steel bar to yield in the fourth time step and reached the midspan section after 22 time steps. The steel stresses in the two vertical reinforcing bars, which tie the roof slab into the vertical walls, are plotted as functions of time in Fig. 6.20. Initially, these two bars provide a fixed-end moment, but as the vertical pressure tends to lift the roof off its supports, also the tensile stress in the left bar builds up. Concrete stresses were not critical at any time of the analysis. The combination of flexure with axial tension forced the reinforcing steel to resist most of the load.

The analysis results lead to the conclusion that the tunnel roof is not likely to survive a gas explosion with the pressure history assumed in Fig. 6.15. The weakest detail appears to be the amount of vertical reinforcement which cannot prevent the vertical pressure from lifting the roof off its supports. Also, the large rotations in the plastic hinges above the support and at midspan are associated with midspan deflections as large as 28.5 cm after 150 time steps (0.1875 sec), which can only be interpreted as failure.

### 6.6.3 Cyclic Response of Reinforced Cantilever Beams

The response of reinforced concrete frame elements to severe cyclic loading has been studied extensively. Comprehensive series of tests were performed in several laboratories, for example the University of California at Berkeley, the University of Illinois at Urbana, and the University of Michigan. Several computer programs are now available, which can simulate this response numerically. Figure 6.21 shows the load-deflection curve of a beam tested by Hwang (1982), compared with the numerical results obtained by program SARCF (Chung 1988; Chung et al. 1988). As can be seen, the strength degradation discussed earlier is reproduced quite well, and so is the pinched shape of the hysteresis loops in the presence of high shear forces. Efforts are under way to further refine the computer models for frame elements and to calibrate them against known experimental response of reinforced concrete building models.

## 6.7 Conclusions

The nonlinear dynamic analysis of reinforced concrete structures belongs to the most difficult tasks facing an engineer. Although a considerable body of knowledge exists on how concrete structures respond to both dynamic and cyclic loads, mathematical models proposed to simulate this behavior are only slowly maturing to the point where they can be applied with confidence to real structures. Often they are calibrated against experimental data over a rather limited parameter range, so that their applicability outside this range is questionable.

As for practical application of these models, the caveats that apply to *any* finite element analysis apply even more so here, because it is very difficult to verify the analysis results by independent means. Experimental test data should be

used wherever possible for benchmark comparisons. Then, with proper caution and engineering judgment, this new analysis tool can be used to study relatively economically the behavior of concrete structures under dynamic load.

## 6.8 References

ACI-ASCE Committee 442 (1988), "Response of Concrete Buildings to Lateral Forces", American Concrete Institute, Detroit, Report 442R-88.

Ad-Hoc Subcommittee on Inelastic Response of Concrete Structures (1991), "Inelastic Response and Design of Earthquake-Resistant Concrete Structures", ACI-ASCE Committee 442, American Concrete Institute, Detroit.

"Computational Mechanics of Concrete Structures, Advances and Applications," IABSE Colloquium, Final Report, Delft, 1987.

Anderson, J.C. and W.H. Townsend (1977), "Models for RC Frames with Degrading Stiffness", ASCE, Journal of the Structural Division, Vol 103, No ST12, Dec.

Banon, H., J.M. Biggs, and H.M. Irvine (1981), "Seismic Damage in Reinforced Concrete Frames", ASCE, Journal of the Structural Division, Vol 107, No ST9, Sept.

Bathe, K.-J. (1982), "Finite Element Procedures in Engineering Analysis", Prentica-Hall, Englewood Cliffs, New Jersey.

Bazant, Z.P. and T.B. Belytschko (1985), "Wave Propagation in a Strain Softening Bar: Exact Solution", Journal of Engineering Mechanics, ASCE, Vol 111, pp 381-389.

Bazant, Z.P. and J. Ozbolt (1989), "Nonlocal Microplane Model for Fracture, Damage, and Size Effect in Structures", Journal of Engineering Mechanics, ASCE, Vol. 116, No. 11, Nov.

Belytschko, T.B. and Z.P. Bazant (1984), "Strain Softening Materials and Finite Element Solutions", *Constitutive Equations - Macro and Computational Aspects*, ASME, pp 253-272.

Bicanic, N. (1978), "Nonlinear Finite Element Transient Analysis of Concrete Structures", Ph.D. Thesis, C/Ph/50/78, University College of Swansea, Wales.

Bicanic, N. and O.C. Zienkiewicz (1983), "Constitutive Model for Concrete Under Dynamic Loading", Earthquake Engineering and Structural Dynamics, Vol. 11, pp. 689-711.

de Borst, R. et al (1983), "DIANA - A Comprehensive but Flexible Finite Element System", *Finite Element Systems Handbook*, 3rd Edition, Springer Verlag, Berlin, Germany.

de Borst, R. and P. Nauta (1985), "Non-Orthogonal Cracks in a Smeared Finite Element Model", Engineering Computations, Vol 2, pp 35-46.

de Borst, R. and J.G. Rots (1989), "Occurrence of Spurious Mechanisms in Computations of Strain-Softening Solids", Engineering Computations, Vol 6, pp 272-280.

Bruhwiler, E. (1990), "Fracture of Mass Concrete Under Simulated Seismic Action", Dam Engineering, Vol. 1, No. 3, pp. 153-176.

Cervenka, V. (1989), "Constitutive Model for Cracked Reinforced Concrete Under General Load Histories", Report, Building Research Institute, Technical University of Prague.

Chappuis, P. and H. Bachmann (1988), "Concrete Material Model Including Strain Rate and Loading History", European Earthquake Engineering, Vol. 1, pp. 22-33.

Chen,E.S. and Buyukozturk,O. (1985), "Constitutive Model for Concrete in Cyclic Compression," Journal of Engineering Mechanics, ASCE, Vol. 111, No. EM6, June, pp. 797-814.

Chen, W.F. (1982), "Plasticity in Reinforced Concrete", McGraw-Hill Book Company, New York.

Chung, Y.S. (1988), "Automated Seismic Analysis and Design of Reinforced Concrete Frames", Ph.D. Thesis, Dept. of Civil Engineering, Columbia University, New York.

Chung, Y.S., C. Meyer, and M. Shinozuka (1987), "Seismic Damage Assessment of Reinforced Concrete Members," Technical Report NCEER-87-0022, National Center for Earthquake Engineering Research, State University of New York, Buffalo.

Chung, Y.S., C. Meyer, and M. Shinozuka (1988), "SARCF User's Guide - Seismic Analysis of Reinforced Concrete Frames," Technical Report NCEER-88-0044, National Center for Earthquake Engineering Research, State University of New York, Buffalo.

Chung, Y.S., C. Meyer, and M. Shinozuka (1989), "Modeling of Concrete Damage", ACI Structural Journal, May-June.

Ciampi, V., R. Eligehausen, V.V. Bertero, and E.P. Popov (1982), "Analytical Model for Concrete Anchorages of Reinforcing Bars under Generalized Excitations", Earthquake Engineering Research Center, Report No. EERC 82-23, University of California, Berkeley, Dec.

Clough, R.W. (1966), "Effect of Stiffness Degradation on Earthquake Ductility Requirements", Report No 66-16, Structural Engineering Laboratory, University of California, Berkeley, Oct.

Collins, M.P., F.J. Vecchio, and G. Mehlhorn (1985), "An International Competition to Predict the Response of Reinforced Concrete Panels", Canadian Journal of Civil Engineering, Vol. 12, pp. 624-644.

Darwin, D. and D.A. Pecknold (1976), "Analysis of RC Shear Panels under Cyclic Loading", Journal of the Structural Division, ASCE, Vol 102, No ST2, February.

Delgado-Saavedra, H.E.(1985), "A Rate-Dependent Model for Plain Concrete Under Dynamic Multiaxial Loads", Ph.D. Thesis, Columbia University, New York.

Eligehausen, R., E.P. Popov, and V.V. Bertero (1983), "Local Bond Stress-Slip Relationships of Deformed Bars Under Generalized Excitations," Earthquake Engineering Research Center, Report No. EERC 83-23, University of California, Berkeley.

Emori, K. and W.C. Schnobrich (1981), "Inelastic Behavior of Concrete Frame-Wall Structures", Journal of the Structural Division, ASCE, Vol 107, No ST1, January.

Endo, F. et al (1989), "Model Tests for Evaluation of Seismic Behavior of Reactor Buildings, Part 7, Strain Rate Test (Evaluation)", Annual Meeting of Architectural Institute of Japan, October.

Filippou, F.C. (1986), "A Simple Model for Reinforcing Bar Anchorages Under Cyclic Excitations", ASCE, Journal of Structural Engineering, Vol. 112, No. 7, July.

Filippou, F.C. and A. Issa (1988), "Nonlinear Analysis of Reinforced Concrete Frames Under Cyclic Load Reversals", Earthquake Engineering Research Center Report No. EERC 88-12, University of California, Berkeley.

Filippou, F.C., E.P. Popov, and V.V. Bertero (1983a), "Effects of Bond Deterioration on Hysteretic Behavior of Reinforced Concrete Joints", Earthquake

Engineering Research Center Report No. EERC 83-19, University of California, Berkeley.
Filippou, F.C., E.P. Popov, and V.V. Bertero (1983b), "Modeling of Reinforced Concrete Joints under Cyclic Excitations", ASCE, Journal of Structural Engineering, Vol. 109, No. 11, November.
Geradin, M., M. Hogge, and G. Robert (1987), "Time Integration of Dynamic Equations", *Finite Element Handbook*, H. Kardestuncer, ed., McGraw-Hill, New York, pp 4.72-4.102.
Giberson, M.F. (1969), "Two Nonlinear Beams with Definition of Ductility", Journal of the Structural Division, ASCE, Vol. 95, No. ST2, Feb.
Glemberg, R. (1984), "Dynamic Analysis of Concrete Structures - Constitutive Modeling, Dynamic Substructuring, Computer Implementation", Publ. 84:1, Chalmers University of Technology, Goteborg.
Grzybowski, M. and C. Meyer (1991), "Damage Prediction for Concrete With and Without Fibre Reinforcement", Dept. of Civil Engineering, Columbia University, New York.
Hatano, T. and H. Tsutsumi (1960), "Dynamical Compressive Deformation and Failure of Concrete Under Dynamic Load", Proceedings, Second World Conference on Earthquake Engineering, Tokyo, Vol. 3, pp.1963-1978.
Hawkins, N.M., I. Lin, and T. Ueda (1987), "Anchorage of Reinforcing Bars for Seismic Forces", ACI Structural Journal, Vol. 84, No. 5, Sept.-Oct.
Holmen, J.O. (1982), "Fatigue of Concrete of Constant and Variable Amplitude Loading", *Fatigue of Concrete Structures*, SP-75, American Concrete Institute, Detroit, pp. 71-110.
Hughes, T.J.R. (1983), "An Analysis of Transient Algorithms With Particular Reference to Stability Behavior", *Computational Methods for Transient Analysis*, T. Belytschko and T.J.R. Hughes, eds., Elsevier Science Publishers, Amsterdam, pp 68-155.
Hughes, T.J.R. (1987), "The Finite Element Method - Linear Static and Dynamic Finite Element Analysis", Prentice-Hall, Englewood Cliffs, New Jersey.
Hwang, T.H. (1982), "Effects of Variation in Load History on Cyclic Response of Concrete Flexural Members", Ph.D. Thesis, Dept. of Civil Engineering, University of Illinois, Urbana.
Inoue, N. and N. Suzuki (1991), "Microscopic and Macroscopic Analysis of Reinforced Concrete Framed Shear Walls", International Workshop on Concrete Shear in Earthquakes, T.T.C. Hsu, editor, Houston, TX.
John, R. and S.P. Shah (1990), "Mixed Mode Fracture of Concrete Subjected to Impact Loading", Journal of Structural Engineering, ASCE, Vol. 116, No. 3, March, pp. 585-602.
Kachanov,L.M. (1958), "Time of Rupture Process under Creep Conditions," Izvestia Akademii Nauk, USSR, 8, 26-31 (in Russian).
Karsan, I.D., and J.O. Jirsa (1969), "Behavior of Concrete under Compressive Loadings", ASCE, Journal of the Structural Division, Vol 95, No ST12, Dec.
Keshavarzian, M. and W.C. Schnobrich (1984), "Computed Nonlinear Seismic Response of R/C Frame-Wall Structures", Civil Engineering Studies, Structural Research Series No. 515, University of Illinois at Urbana-Champaign, Urbana, Ill., May.
Kollegger, J. and G. Mehlhorn (1988), "Biaxiale Zug-Druckversuche an Stahlbetonscheiben", Research Report No. 6, Fachgebiet Massivbau, University Kassel, Germany (in German).
Krajcinovic, D. and G.U. Fonseka (1981a), "The Continuous Damage Theory of Brittle Materials. Part 1: General Theory", Journal of Applied Mechanics, Vol. 48, Dec., pp. 809-815.

Krajcinovic, D. and G.U. Fonseka (1981b), "The Continuous Damage Theory of Brittle Materials. Part 2: Uniaxial and Plane Response Modes", Journal of Applied Mechanics, Vol. 48, Dec., pp. 816-824.
Kwak, H.G. and F.C. Filippou (1990), "Finite Element Analysis of Reinforced Concrete Structures Under Monotonic Loads", Report No. 90/14, Structural Engineering, Mechanics and Materials, Department of Civil Engineering, University of California, Berkeley, November.
Lasry, D. and T. Belytschko (1988), "Localization Limiters in Transient Problems", Int. Journal of Solids and Structures, Vol 24, pp 581-597.
Li, K.N., S. Otani and H. Aoyama (1988), "Reinforced Concrete Columns Under Varying Axial Load and Bi-Directional Lateral Load Reversals", Proceedings, 9th World Conference on Earthquake Engineering, Tokyo/Kyoto.
Mahin, S.A. and V.V. Bertero (1972), "Rate of Loading Effects on Uncracked and Repaired Reinforced Concrete Members", Earthquake Engineering Research Center Report No. EERC 72-9, University of California, Berkeley.
Mahin, S.A. and V.V. Bertero (1976), "Problems in Establishing and Predicting Ductility in Aseismic Design", Proceedings International Symposium on Earthquake Structural Engineering, St. Louis, MO, August.
Mazars, J. (1981), "Mechanical Damage and Fracture of Concrete Structures", *Advances in Fracture Research*, Francois, D., ed., Proc. ICFS, Vol. 4, Cannes, France, pp.816-824.
Mazars,J. and Pijaudier-Cabot,G. (1989), "Continum Damage Theory - Application to Concrete," Journal of Engineering Mechanics, ASCE, Vol. 115, No. 2, Feb., pp. 345-365.
Menegotto, M. and P. Pinto (1973), "Method of Analysis for Cyclically Loaded Reinforced Concrete Plane Frames Including Changes in Geometry and Nonelastic Behavior of Elements under Combined Normal Force and Bending", IABSE Symposium on Resistance and Ultimate Deformability of Structures Acted on by Well-Defined Repeated Loads, Final Report, Lisbon.
Meyer, C., ed. (1987a), "Finite Element Idealization", Special Publication, ASCE, New York.
Meyer, C. (1987b), "Analysis of Underwater Tunnel for Internal Gas Explosion", IABSE Colloquium on Computational Mechanics of Concrete Structures, Delft, The Netherlands.
Meyer, C. (1991), "Reinforced COncrete Frames Subjected to Cyclic Load", *Structures Subjected to Repeated Loading - Stability and Strength*, Elsevier Science Publishers, London.
Meyer, C. and H.E. Delgado-Saavedra (1986), "Modeling Large Inelastic Cyclic Response of Concrete", Proceedings, U.S.-Japan Seminar, Tokyo, Special Publication, ASCE.
Meyer, C. and H. Okamura, eds (1985), "Finite Element Analysis of Reinforced Concrete," Special Publication, ASCE, New York.
Meyer, C., M.S. Roufaiel, and S.G. Arzoumanidis (1983), "Analysis of Damaged Concrete Frames for Cyclic Loads", Earthquake Engineering and Structural Dynamics, Vol. 11, pp. 207-228.
van Mier, J.G.M. (1987), "Examples of Non-Linear Analysis of Reinforced Concrete Structures with DIANA", Heron, Vol. 32, No. 3, Delft, The Netherlands.
Naeim, F., ed. (1989), "The Seismic Design Handbook", Van Nostrand Reinhold, New York.
Needleman, A. (1988), "Material Rate Dependence and Mesh Sensitivity in Localization Problems", Comp. Meth. Appl. Mech. Eng., Vol 67, pp 69-86.
Nilson, A.H., ed. (1982), "Finite Element Analysis of Reinforced Concrete", Special Publication, ASCE, New York.

Nilsson, L. (1978), "Finite Element Analysis of Impact on Concrete Structures", *Finite Elements in Nonlinear Mechanics*, P. Bergan et al, eds., Tapir, Trondheim.
Nilsson, L. and R. Glemberg (1981), "A Constitutive Model for Concrete in High Rate of Loading Conditions", Proceedings, IABSE Colloquium, Delft, pp. 159-174.
Noguchi, H. (1985), "Analytical Models For Cyclic Loading of Reinforced Concrete Members", *Finite Element Analysis of Reinforced Concrete Structures*, C. Meyer and H. Okamura, eds, ASCE, New York.
Oh, B.H. (1991), "Cumulative Damage Theory of Concrete under Variable-Amplitude Fatigue Loadings", ACI Materials Journal, January-February.
Okada, T. et al (1989), "Model Tests for Evaluation of Seismic Behavior of Reactor Buildings", Part 1-5, Annual Meeting of the Architectural Institute of Japan, October.
Otani, S. (1974), "Inelastic Analysis of R/C Frame Structures", ASCE, Journal of the Structural Division, Vol 100, No ST7, July.
Otani, S., K. Kitayama, and H. Aoyama (1985), "Beam Bar Bond Stress and Behaviour of Reinforced Concrete Interior Beam-Column Joints", Second US-NZ-Japan Seminar on Design of Reinforced Concrete Beam-Column Joints, Tokyo, Japan, May 29-30.
Park, Y.J. and A.H.S. Ang (1985), "Mechanistic Seismic Damage Model for Reinforced Concrete", Journal of Structural Engineering, ASCE, Vol. 111, No. 4, April.
Park, K.C. and C.A. Felippa (1983), "Partitioned Analysis of Coupled Systems", *Computational Methods for Transient Analysis*, T. Belytschko and T.J.R. Hughes, eds., Elsevier Science Publishers, Amsterdam, pp 158-219.
Park, R. and T. Paulay (1975), "Reinforced Concrete Structures", John Wiley and Sons, New York.
Park, R. and T. Paulay (1984), "Joints in Reinforced Concrete Frames Designed for Earthquake Resistance," Research Report 84-9, Department of Civil Engineering, University of Canterbury, Christchurch, June.
Perzyna, P. (1966), "Fundamental Problems in Viscoplasticity", Advances in Applied Mechanics, Vol. 9, pp. 243-377.
Powell, G.H. (1991), Private Communication.
Paulay, T. and M.J.N. Priestley, "Seismic Design of Reinforced Concrete and Masonry Buildings", John Wiley and Sons, New York, 1992.
Read, H.E. and G.A. Hegemier (1984), "Strain Softening of Rock, Soil and Concrete - A Review Article", Mechanics of Materials, Vol 3, pp 271-294.
Reinhardt, H.W. (1986), "Strain Rate Effects on the Tensile Strength of Concrete as Predicted by Thermodynamic and Fracture Mechanics Models", *Cement Based Composites: Strain Rate Effects and Fracture*, S. Mindess and S.P. Shah, eds., MRS Symposium, Proceedings, No. 64, Pittsburgh.
Reinhardt, H.W., H.A.W Cornelissen, and D.A. Hordijk (1986), "Tensile Tests and Failure Analysis of Concrete", Journal of Structural Engineering, ASCE, Vol 112, pp 2462-2477.
Reitherman, R. (1985), "A Review of Earthquake Damage Estimation Methods," Earthquake Spectra, EERI, Vol. 1, No. 4, August.
Riggs, H.R. and G.H. Powell (1986), "Rough Crack Model for Analysis of Concrete", Journal of Engineering Mechanics, ASCE, Vol. 112, No. 5, May.
Rots, J.G. (1988), "Computational Modeling of Concrete Fracture", Dissertation, Delft University of Technology, Delft.
Roufaiel, M.S.L. and C. Meyer (1987), "Analytical Modeling of Hysteretic Behavior of R/C Frames", Journal of Structural Engineering, ASCE, Vol. 113, No.

3, March.
Saiidi, M. (1982), "Hysteresis Models for Reinforced Concrete", Journal of the Structural Division, ASCE, Vol. 108, No. ST5, May.
Sandler, I.S. (1984), "Strain Softening for Static and Dynamic Problems", *Constitutive Equations - Macro and Computational Aspects*, ASME, pp 217-231.
Schreyer, H.L. and Z. Chen (1986), "One-Dimensional Softening with Localization", Journal of Applied Mechanics, ASME, pp 217-231.
Shah, S.P., ed. (1982), "Fatigue of Concrete Structures", ACI Special Publication SP-75.
Sluys, L.J. (1989a), "Strain Softening Under Static and Dynamic Loading Conditions", TU-Delft Report No. 25.2.89.5.09, Delft University of Technology, Delft.
Sluys, L.J. (1989b), "Numerical Analyses of Impact Tensile Tests on Concrete", TU-Delft Report No. 25.2.89.5.15, Delft University of Technology, Delft.
Sluys, L.J. (1990), "Localization in a Cosserat Continuum Under Dynamic Loading Conditions", TU-Delft Report No. 25.2.90.5.15, Delft University of Technology, Delft.
Sluys, L.J. and R. de Borst (1990a), "Strain Softening Under Dynamic Loading Conditions", *Computer Aided Analysis and Design of Concrete Structures*, N. Bicanic and H.A. Mang, eds., Pineridge Press, Swansea, pp 1091-1104.
Sluys, L.J. and R. de Borst (1990b), "A Numerical Study of Concrete Fracture Under Impact Loading", *Micromechanics of Failure of Quasi-Brittle Materials*, S.P. Shah et al, eds., Elsevier Applied Science, London, pp 524-535.
Soleimani, D., E.P. Popov, and V.V. Bertero (1979), "Nonlinear Beam Model for R/C Frame Analysis", 7th ASCE Conference on Electronic Computation, St. Louis, MO, August.
Song, C.M. and K. Maekawa (1991), "Dynamic Nonlinear Finite Element Analysis of Reinforced Concrete", Journal of the Faculty of Engineering, The University of Tokyo (B), Vol. XLI, No. 1.
Stevens, N.J., S.M. Uzumeri, and M.P. Collins (1987), "Analytical Modeling of Reinforced Concrete Subjected to Monotonic and Reversed Loadings", Report No. 87-1, Department of Civil Engineering, University of Toronto.
Suaris, W. and V. Fernando (1987), "Ultrasonic Pulse Attenuation as a Measure of Damage Growth During Cyclic Loading of Concrete", ACI Materials Journal, May-June.
Suaris, W., and Shah, S. P. (1984), "Rate-Sensitive Damage Theory for Brittle Solids", Journal of Engineering Mechanics, ASCE, Vol. 110, No. 6, June, pp. 985-997.
Suaris, W., and Shah, S. P. (1985), "Constitutive Model for Dynamic Loading of Concrete", Journal of Engineering Mechanics, ASCE, Vol. 111, No. 3, March, pp. 563-576.
Takayanagi, T. and W.C. Schnobrich (1979), "Non-Linear Analysis of Coupled Wall Systems", Earthquake Engineering and Structural Dynamics, Vol. 7, pp. 1-22.
Takeda, T., M.A. Sozen, and N.N. Nielsen (1970), "Reinforced Concrete Response to Simulated Earthquakes", Journal of the Structural Division, ASCE, Vol 96, No ST12, December.
Tassios, T.P. and P.J. Yannopoulos (1981), "Analytical Studies on Reinforced Concrete Members Under Cyclic Loading Based on Bond Stress-Slip Relationships", ACI Journal, Vol 78, May-June.
Vecchio, F.J. and M.P. Collins (1982), "The Response of Reinforced Concrete to In-Plane Shear and Normal Stresses", Report No. 82-03, Department of Civil Engineering, University of Toronto, March.

Vecchio, F.J. and M.P. Collins (1986), "The Modified Compression-Field Theory for Reinforced Concrete Elements Subjected to Shear", ACI Journal, Vol. 83, No. 2, March-April.
Viwathanatepa, S., E.P. Popov, and V.V. Bertero (1979), "Effects of Generalized Loadings on Bond of Reinforcing Bars Embedded in Confined Concrete Blocks", Earthquake Engineering Research Center Report No. EERC 79-22, University of California, Berkeley, August.
Weerheijm, J. and H.W. Reinhardt (1989), "Concrete in Impact Tensile Tests", Proc., First Int. Conference on Structures under Shock and Impact, Cambridge, Massachusetts.
Willam, K.J. and E.P. Warnke (1974), "Constitutive Model for Triaxial Behavior of Concrete", IABSE Seminar on Concrete Structures Subjected to Triaxial Stresses, Paper III-1, Bergamo, Italy.
Yokoyama, M., K. Mutsuyoshi and A. Machida (1990), "Elasto-Plastic Response of RC Members with Pseudo-Dynamic Procedure", Proceedings, Japan Concrete Institute.
Zeris, C.A. and S.A. Mahin (1988), "Analysis of Reinforced Concrete Beam-Columns under Uniaxial Excitations", Journal of Structural Engineering, ASCE, Vol. 114, No. 4, April.
Zhou, T. et al (1990), "Tri-Axial Nonlinear Analytical Model of Reinforced Concrete Column". Proceedings, Japan Concrete Institute, Vol. 12, No. 2.
Zielinski, A.J. (1982), "Fracture of Concrete and Mortar Under Uniaxial Impact Tensile Loading", Dissertation, Delft University of Technology, Delft.

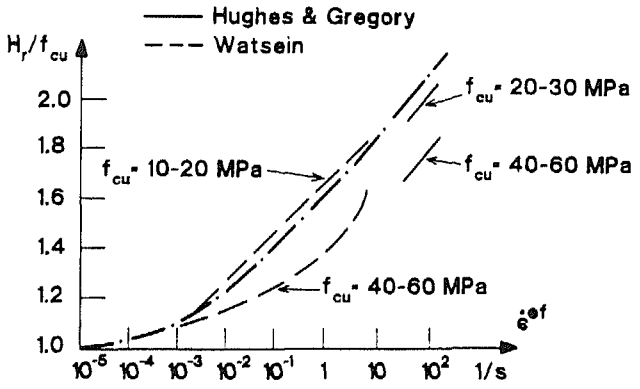


Fig. 6.1 Effect of Average Strain Rate On Compressive Strength of Concrete

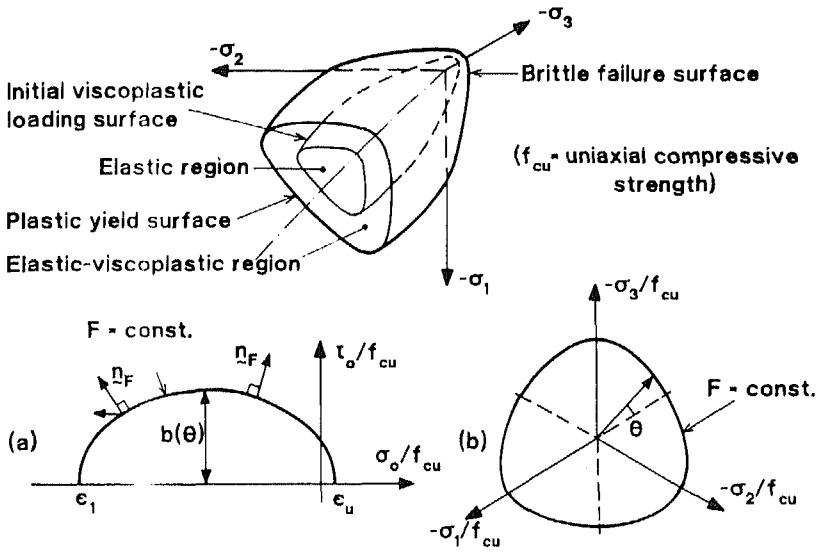


Fig. 6.2 Regions of Elasticity, Viscoplasticity, Plasticity, and Brittle Failure

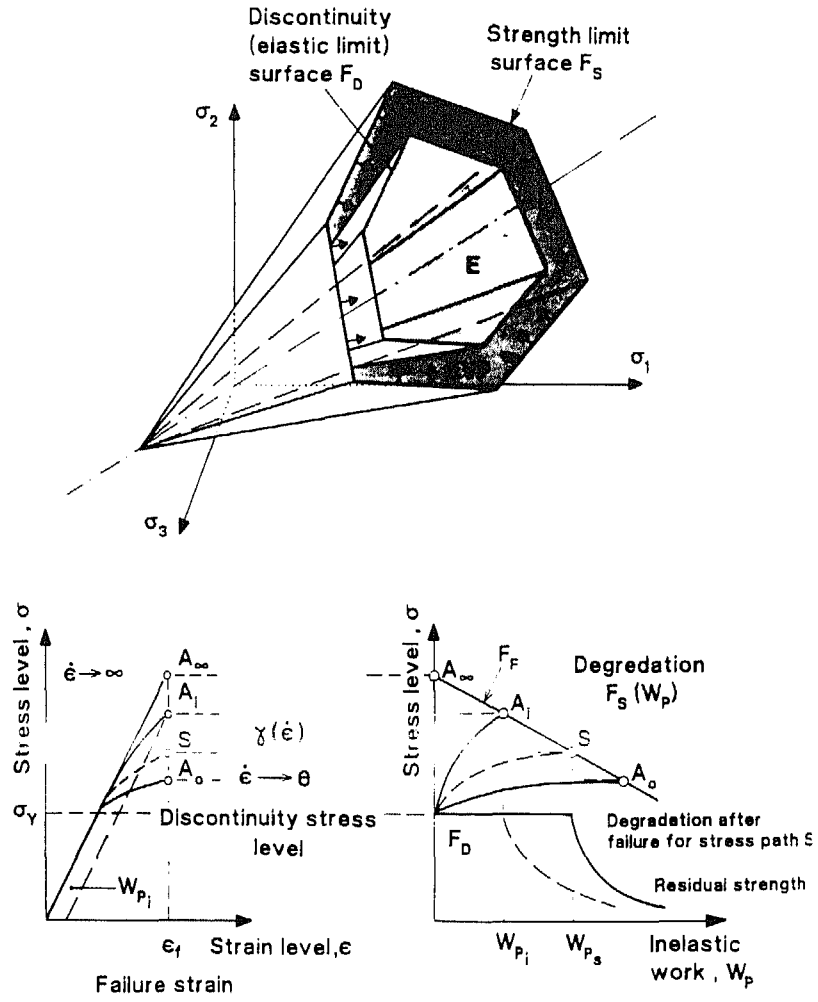
Discontinuity
(elastic limit)
surface $F_D$
Strength limit
surface $F_S$
$\sigma_2$
E
$\sigma_1$
$\sigma_3$
Stress level, σ
$\dot{\epsilon} \to \infty$
$A_\infty$
$A_i$
S
$A_o$
$\gamma(\dot{\epsilon})$
$\dot{\epsilon} \to 0$
$\sigma_Y$
Discontinuity stress level
$W_{P_i}$
$\epsilon_f$
Strain level, ϵ
Failure strain
Stress level, σ
$A_\infty$
$F_F$
Degredation
$F_S(W_P)$
$A_i$
S
$A_o$
Degradation after failure for stress path S
$F_D$
Residual strength
$W_{P_i}$
$W_{P_s}$
Inelastic work, $W_P$

Fig. 6.3

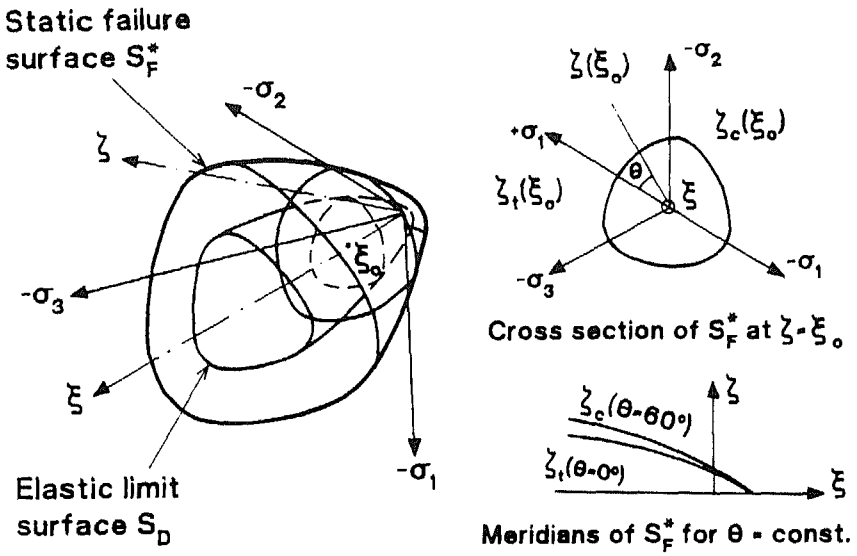


Fig. 6.4 Geometry of Static Failure Surface $S_F^*$ and Elastic Limit Surface $S_D$

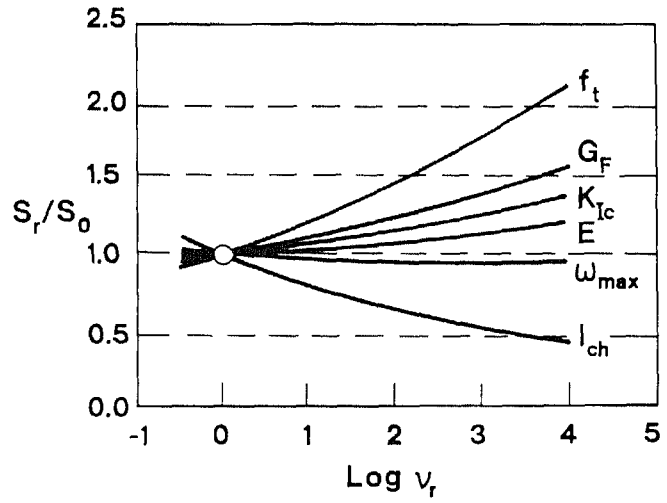


Fig. 6.5 Effect of Deformation Rate on Fracture Properties of Concrete

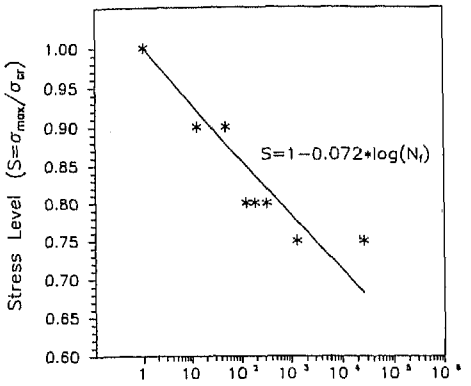


a) Plain concrete

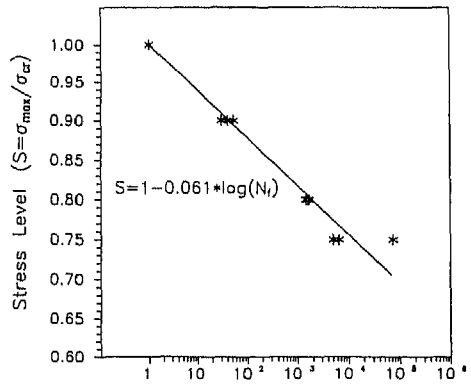


b) 0.5% polypropylene fibre

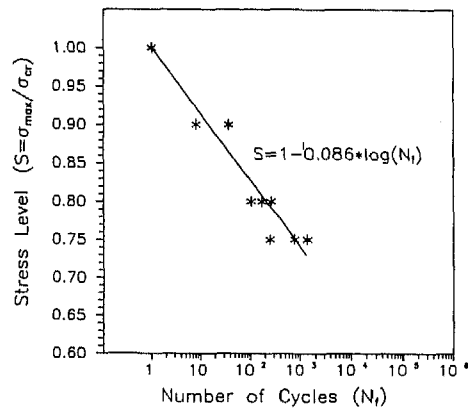


c) 0.5% steel fibre

Fig. 6.6 S-N Curves

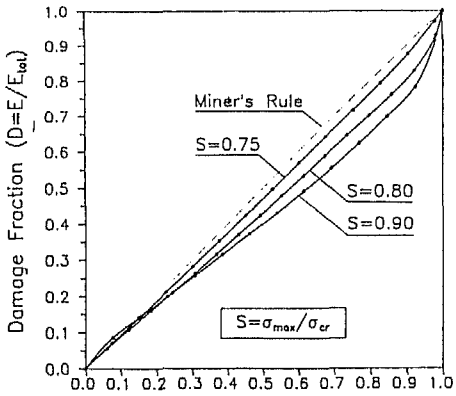


a) Plain concrete

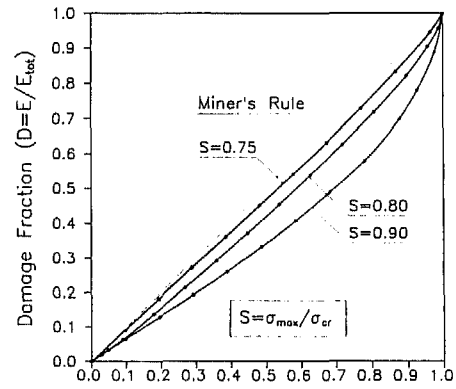


b) 0.5% polypropylene fibre

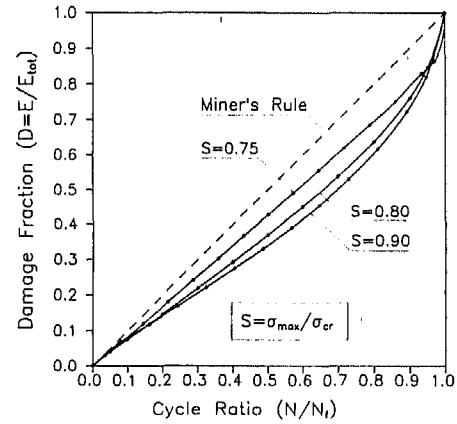


c) 0.5% steel fibre

Fig. 6.7 Damage Accumulation Curves

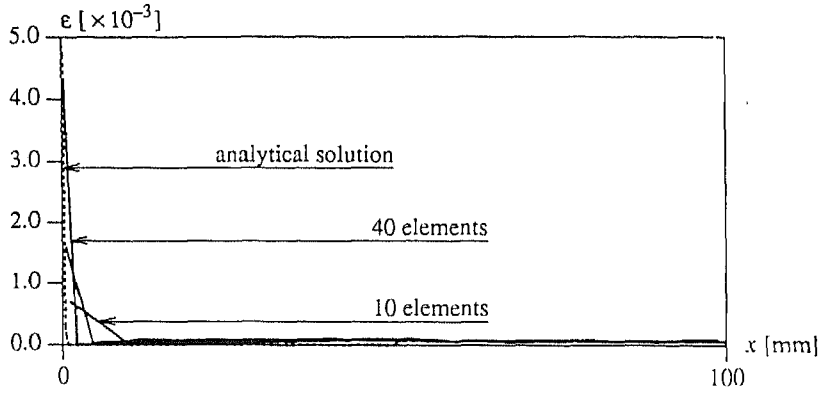


Fig. 6.8 Mesh-Dependent Results With Classical Strain-Softening Model: Strain Localization Along the Bar at $t = \frac{3}{2}\frac{L}{c_e} = 0.15 \times 10^{-3}$ *sec.*

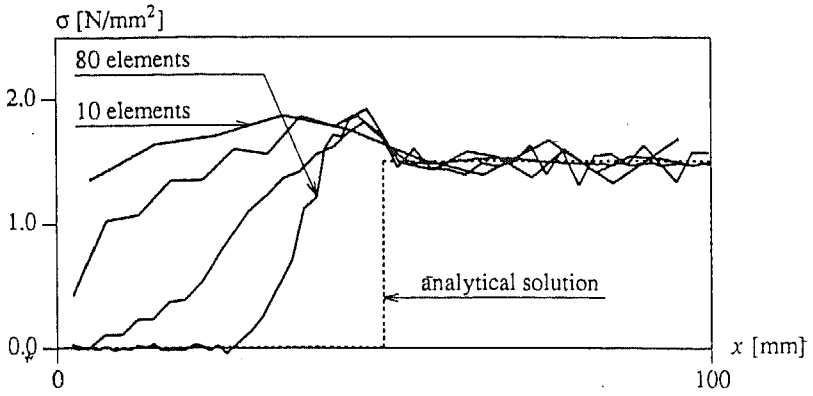


a) Stress profiles along the bar at $t = \frac{3}{2}\frac{L}{c_e} = 0.15 \times 10^{-3}\ sec$

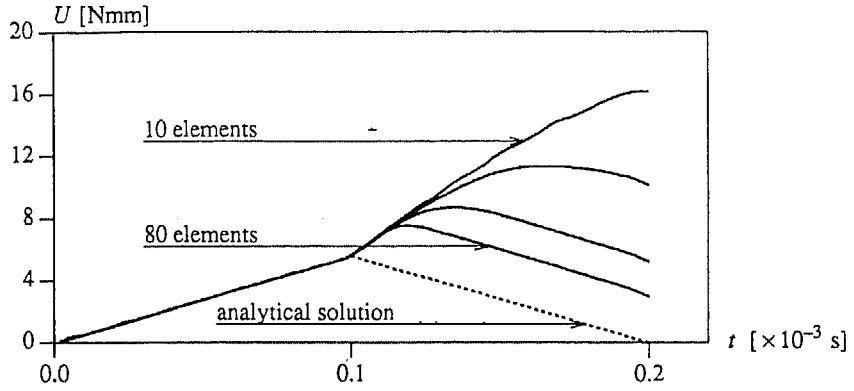


b) Energy consumption of the bar

Fig. 6.9 Mesh-Dependent Results With Classical Strain-Softening Model

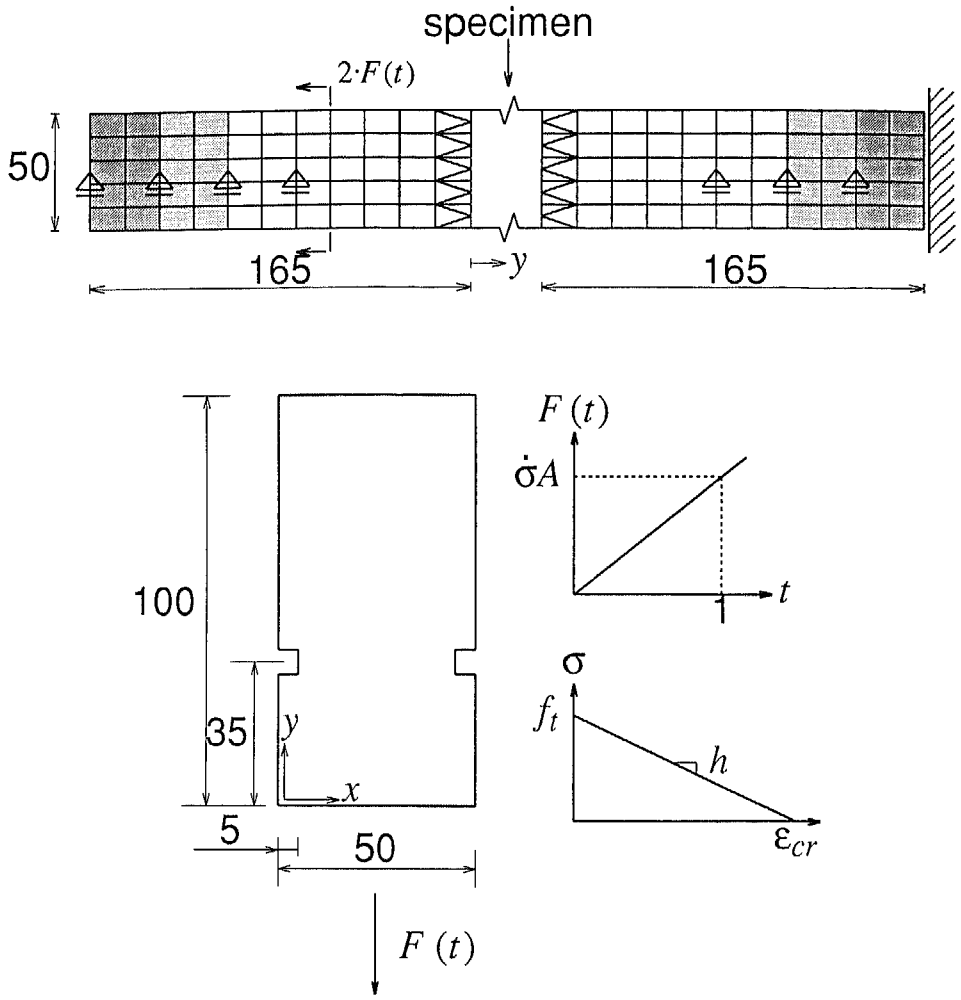


Fig. 6.10 Numerical Model of Test Set-Up

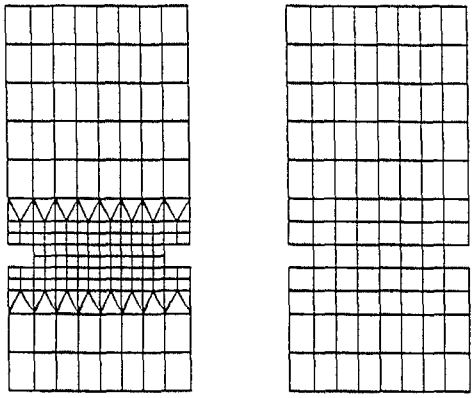

a) Fine mesh b) Coarse mesh

Fig. 6.11 Finite Element Configurations

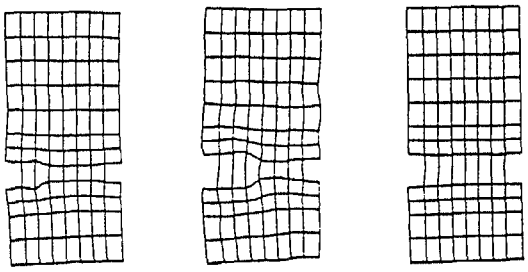

a) After crack initiation b) Pre-peak situation c) At-peak situation

Fig. 6.12 Incremental Displacement Fields

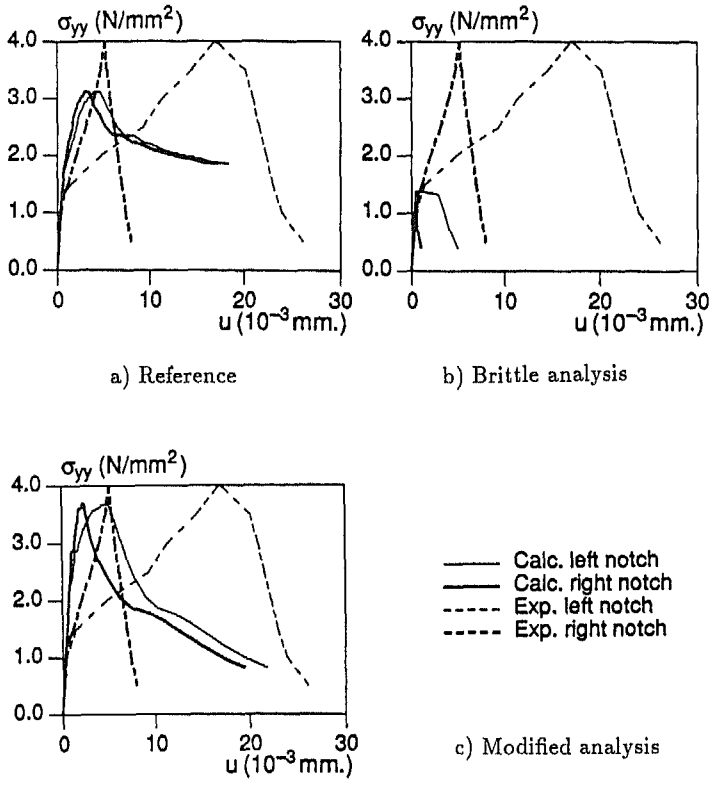


a) Reference

b) Brittle analysis

c) Modified analysis

Fig. 6.13 Stress-Deformation Curves Inside Fracture Zone

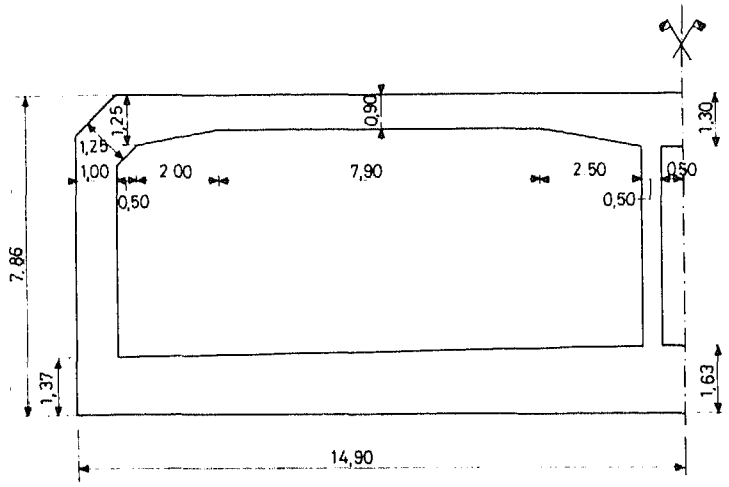


a) Cross-sectional dimensions

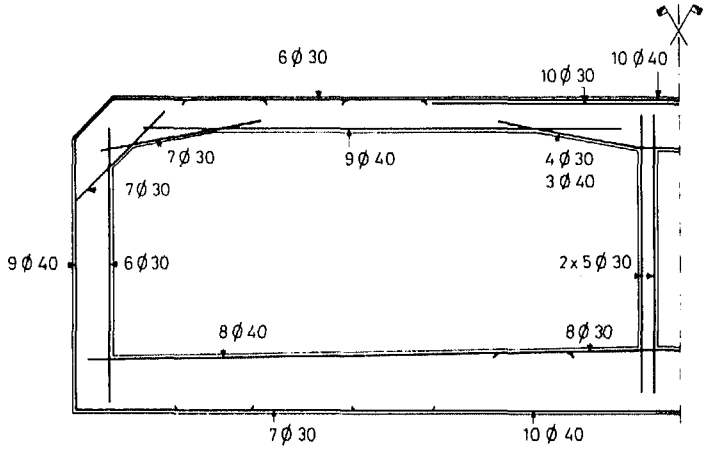


b) Reinforcement for a 1.5 m wide section

| Concrete | | | Reinforcing Steel | | |
|---|---|---|---|---|---|
| $E_c =$ | 22,000 | $N/mm^2$ | $E_s =$ | 210,000 | $N/mm^2$ |
| $\nu =$ | 0.2 | | $f_y =$ | 528 | $N/mm^2$ |
| $f'_t =$ | 3.36 | $N/mm^2$ | | | |
| $f'_c =$ | 30 | $N/mm^2$ | | | |
| $\epsilon_{tu} =$ | 0.001 | | | | |

c) Material properties

Fig. 6.14 Under-Water Tunnel

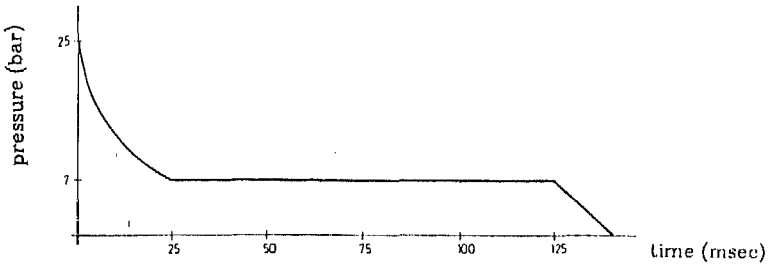


Fig. 6.15 Assumed Pressure Time History

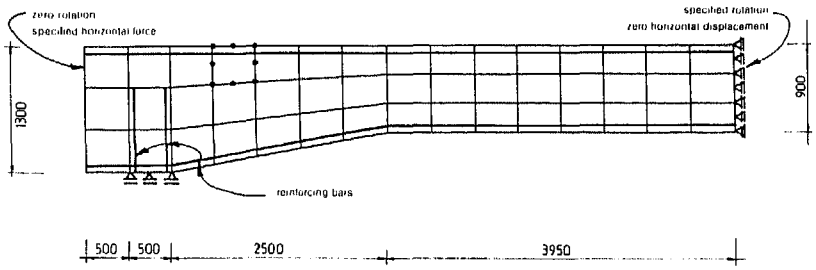


Fig. 6.16 Finite Element Model for Tunnel Roof (Dimensions in $mm$)

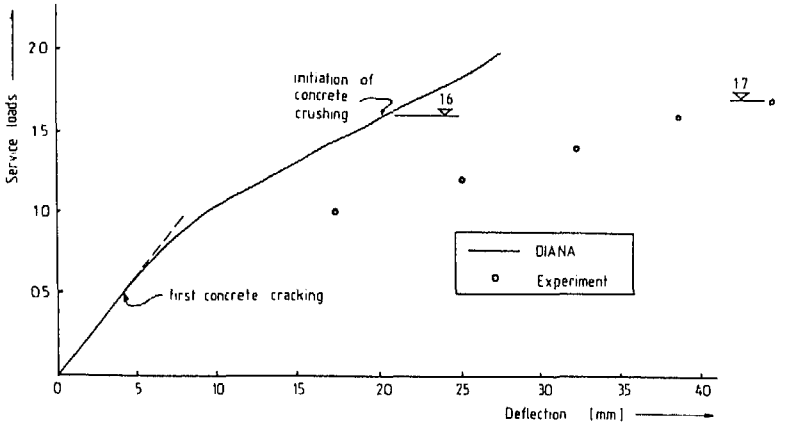


Fig. 6.17 Experimental and Analytical Load-Deflection Behavior

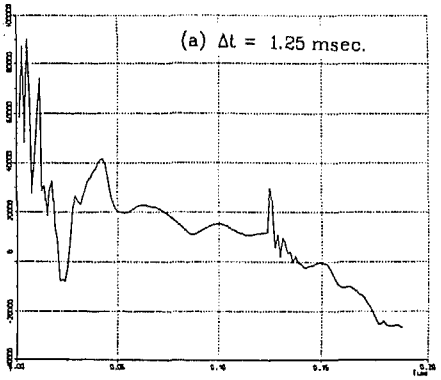


a) Accelerations ($mm/sec^2$)

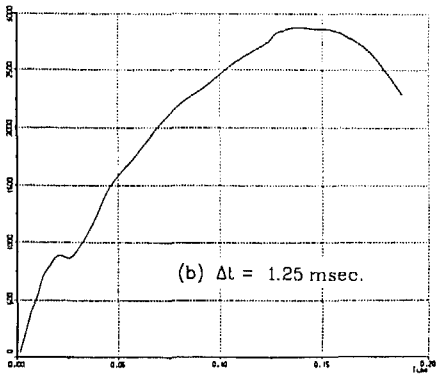


b) Velocities ($mm/sec$)

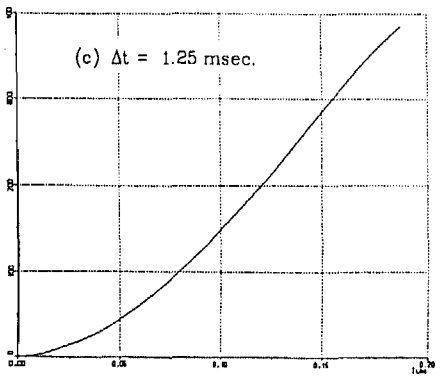


c) Displacements ($mm$)

Fig. 6.18 Time History Response of Tunnel Roof at Midspan

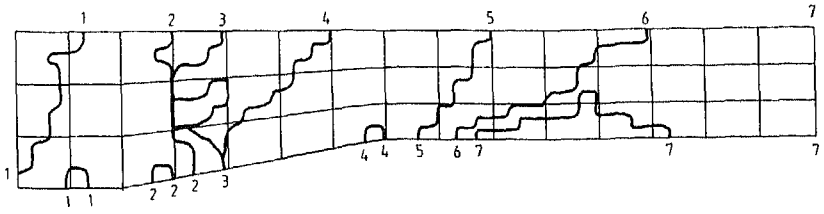

Fig. 6.19 Propagation of Concrete Cracking Wave Front
(Numbers indicate number of time steps of 1.25 *msec*)

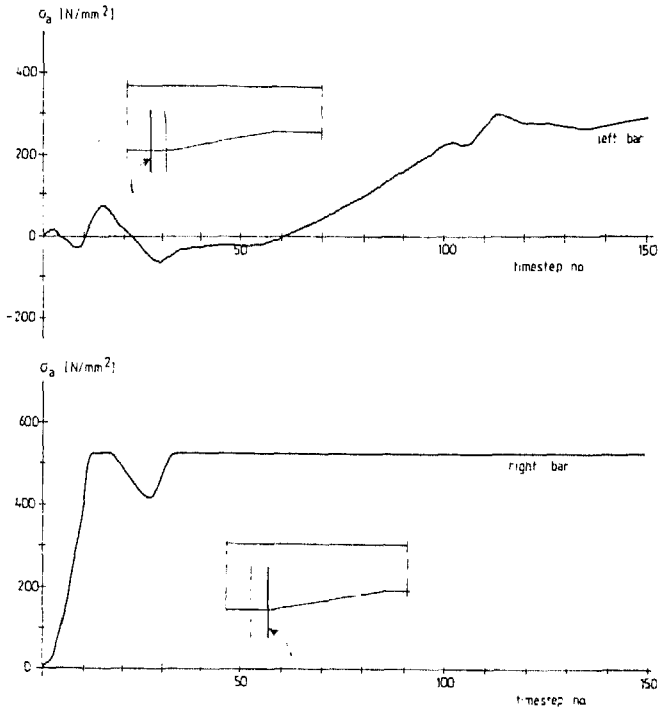


Fig. 6.20 Time Histories of Stresses in Vertical Reinforcing Bars